

SUSCEPTIBILITY OF DILUTE LA-GD ALLOYS

by

Nicholas Theodore Panousis

A Thesis Submitted to the
Graduate Faculty in Partial Fulfillment of
The Requirements for the Degree of
MASTER OF SCIENCE

Major Subject: Physics

Signatures have been redacted for privacy

Iowa State University
Of Science and Technology
Ames, Iowa

1965

TABLE OF CONTENTS

	Page
I. INTRODUCTION AND THEORY	1
II. SAMPLES	10
III. APPARATUS	11
A. Temperature Control and Measurement	11
B. Magnetometer	13
C. Magnetic Field	16
IV. CALCULATIONS AND RESULTS	18
A. Calibration	18
B. Calculation of the Susceptibilities and Curie Temperatures	19
C. Calculation of Effective Bohr Magnetons and Curie Constants	37
D. Calculation of the Weiss Constants and Molecular Fields	42
V. SUMMARY AND CONCLUSIONS	43
VI. BIBLIOGRAPHY	45
VII. ACKNOWLEDGEMENTS	48

1. INTRODUCTION AND THEORY

Susceptibility measurements have long been an effective tool for the investigation of magnetic substances. While this technique can not give direct information about the microscopic structure of the material, it can point the way toward reasonable models and provide guide lines for possible theories. In the cases where models give explicit relations for the temperature and magnetic field dependence of the susceptibility, these measurements provide an easy check on the validity of the proposed pictures.

One of the best established theories of paramagnetism is the Curie-Weiss model. Within the framework of this theory atoms are considered to have dipole moments which are free to orient under the constraints of the temperature of the sample and the local magnetic field at the site of the atom. In zero applied field the dipole moments are assumed to be randomly oriented due to thermal agitation. The application of an external magnetic field alters this distribution and produces a net alignment of the moments in the applied field direction. This net magnetic moment per unit volume is called the magnetization, M . For a system of N non-interacting paramagnetic atoms per unit volume, an application of quantum statistical mechanics yields for the magnetization (7).

$$M = N g J \mu_B B_J (X) \quad (1)$$

where g is the Lande splitting factor given by

$$g = 1 + \frac{J(J+1) - L(L+1) + S(S+1)}{2J(J+1)} \quad (2)$$

and J , L and S are the total, orbital, and spin quantum numbers respectively
 μ_B is the Bohr magneton given by

$$\mu_B = \frac{e h}{4\pi m c} = 0.927 \times 10^{-20} \frac{\text{erg}}{\text{gauss}} \quad (3)$$

and $B_J(X)$ is the Brillouin function (4) given by

$$B_J(X) = \frac{2J+1}{2J} \coth \frac{(2J+1)X}{2J} - \frac{1}{2J} \coth \frac{X}{2J} \quad (4)$$

for X given by

$$X = \frac{g J \mu_B H}{k T} \quad (5)$$

where H is the applied magnetic field corrected for demagnetization effects,
 k is Boltzmann's constant, and T is absolute temperature.

In the case where $X \ll 1$, Equation 1 reduces to

$$\chi = \frac{M}{H} = \frac{N g^2 J(J+1) \mu_B^2}{3 k T} \quad (6)$$

$$\chi = \frac{C}{T} \quad (7)$$

where

$$C = \frac{N g^2 J(J+1) \mu_B^2}{3 k} \quad (8)$$

Equation 6 or 7 is known as the Curie law for paramagnetic susceptibility
and Equation 8 defines the Curie constant.

It is observed that many paramagnetic materials have a susceptibility behavior similar to, but not quite, that predicted by Equation 7. The deviations from the simple Curie law arise from the fact that the magnetic dipoles are not free but rather are coupled together. The first successful attempt to incorporate the dipole coupling into the theory is due to Weiss (34). He reasoned that the net field acting on an ion is the applied field plus a field proportional to the magnetization given by

$$H_m = H_a + \lambda M \quad (9)$$

where λ is called the molecular field or Weiss constant. This additional field then incorporates the effects of coupling.

By use of the molecular field modification, Equation 9, one can recalculate the expression for the susceptibility. The result obtained (7),

$$\chi = \frac{C}{T - \theta} \quad (10)$$

is known as the Curie-Weiss law. Comparison of Equations 7 and 10 shows that the Weiss modification introduces a new quantity into the susceptibility expression. This quantity is called the Curie temperature (more correctly the paramagnetic Curie temperature) and can be expressed as (7)

$$\theta = \frac{\lambda N g^2 J(J+1) \mu_B^2}{3 k} = C \lambda \quad (11)$$

Its meaning is obtained as follows. From Equation 10 a plot of the reciprocal of the susceptibility against temperature is a straight line. The Curie temperature is then obtained by extrapolating this line to the

temperature axis. A positive value of θ is interpreted as indicating ferromagnetic coupling characterized by parallel alignment of the individual moments. Similarly, a negative value of θ is interpreted as an indication of antiferromagnetic coupling characterized by anti-parallel alignment of the individual moments. This behavior is shown schematically in Figure 1.

Another quantity of interest is the effective magnetic moment per atom, P_{eff} . Within the framework of this model P_{eff} is given by (7).

$$P_{\text{eff}} = g [J(J + 1)]^{1/2} \quad (12)$$

$$P_{\text{eff}} = \left[\frac{3 k (T - \theta) \chi}{N \mu_B^2} \right]^{1/2} \quad (13)$$

This quantity is considered further below but we mention here that deviations from the free ion value can be interpreted as a measure of the conduction electron-ion interaction. Observed values of P_{eff} larger or less than the free ion contribution are interpreted to give the sign of the conduction electron polarization.

The Curie-Weiss theory is general and provides only limited insight into the details of the coupling. More recently extensive theoretical work has shown that this polarization may arise from the interactions between the conduction electrons and the magnetic impurity ions. In this work we are interested in the magnetic properties of Gd dissolved in La. Therefore, we take this case to illustrate qualitatively the model for the conduction electron-ion interaction. The 4-f electrons of the Gd ion interact with the s-band conduction electrons through the

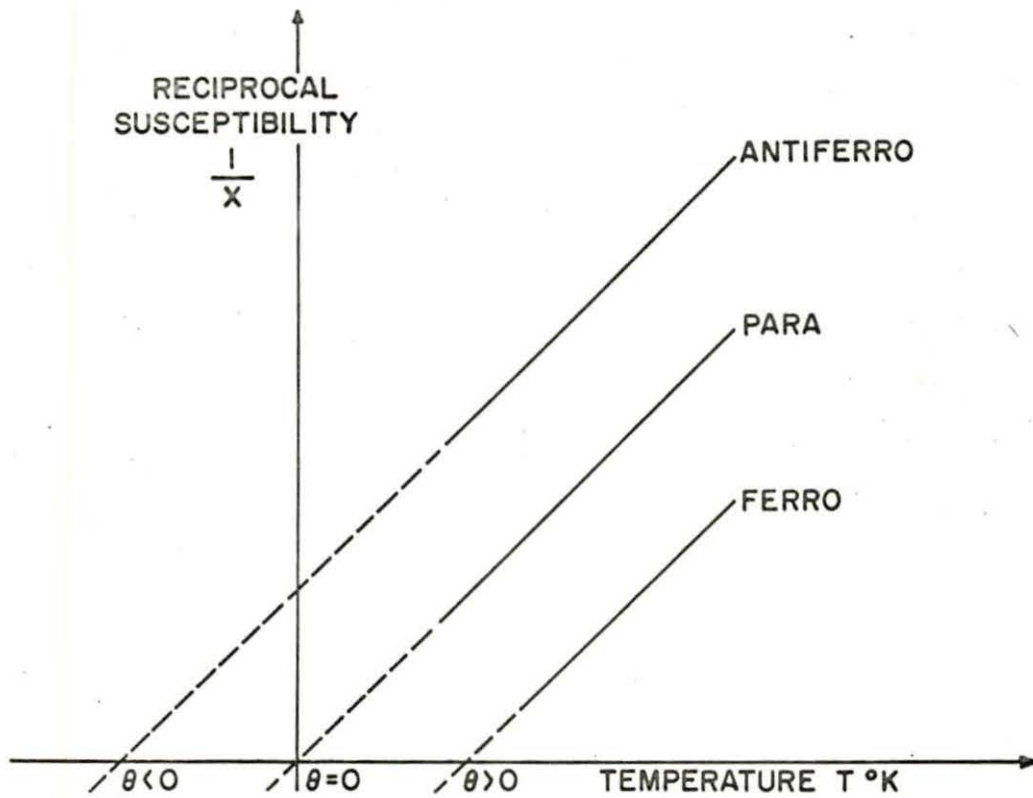
SCHEMATIC REPRESENTATION OF THREE TYPES
OF MAGNETIC BEHAVIOR

Figure 1. Schematic representation of three types of magnetic behavior

electrostatic coulomb exchange. This interaction tends to align the spins of the conduction electrons either parallel or antiparallel to the spin of the trivalent Gd ion. Therefore, the conduction electron spins are no longer randomly oriented and further interaction produces a net polarization.

In this experiment the method used to determine the net polarization is the determination of the number of effective Bohr magnetons. At the suggestion of van Vleck (33), an agreement with the value for the free ion is interpreted to mean the ion under consideration is essentially free. A larger value indicates a net polarization of conduction electrons parallel to the magnetic impurity ion¹. Similarly, a smaller value indicates a net negative or antiparallel polarization of the conduction electrons relative to the impurity ion.

These ideas have previously been applied to magnetic alloy systems. Owen et al. (19, 20) considered the system of Mn dissolved in Cu. They conclude that (1) the s-d interaction was at least a factor of 10 weaker than expected, (2) the Curie temperatures increased approximately linearly with Mn content over the range of 0.03 to 11.1 atomic percent, and (3) an antiferromagnetic transition was observed at low temperatures. Also to be noted is that the results they report were corrected for the host contribution. This was accomplished by subtracting the susceptibility of Cu (-0.76×10^{-6} emu) from the observed values.

Crangle (6) has considered the system of Gd dissolved in Pd. The relevant conclusions of his work are (1) the Curie temperatures varied in

¹Sugawara (30, 31) also suggests this interpretation but warns that it could be due simply to clustering of the impurity ions.

an approximately linear fashion with Gd concentration over the range of about 1 to 10 atomic percent, (2) the number of effective Bohr magnetons showed a slight tendency to increase with Gd concentration, and (3) the value of the effective Bohr magneton was less than the free ion value and so negative conduction electron polarization is indicated. Note, however, that the results he reports have not been corrected for the host contribution. This may be important for the smallest concentrations of Gd since the susceptibility of pure Pd (7.3×10^{-6} emu) is a factor of 10 larger than for Cu used in Owen's work. This last point is given further consideration in the calculations.

Further evidence for conduction electron polarization is obtained by Jacarrino et al. (11) and Peter et al. (21, 22). They use as their probe the shift in the spectroscopic g-factor which they determine by nuclear and/or electron magnetic resonance. Their results indicate a negative exchange interaction. Since the direct exchange interaction between ion and conduction electron is known to be positive (35), Peter et al. conclude that this simple interaction model¹ is not applicable. A similar conclusion is given by Shaltiel et al. (24) who argue that a net or effective exchange interaction should be considered. Of particular relevance here is their indication that the exchange between Gd and d-electrons will be negative but that for Gd with s-electrons (as for the La host) will be positive.

The results obtained by Thoburn (32) and Nelson (17) are compatible with the above indication of Shaltiel et al. Thorburn considers the system

¹For further detailed models see, for example, Anderson and Clogston (1) and Kodie and Peter (13).

of Gd dissolved in La over the concentration range of 45 to 90 atomic percent. His value for the effective Bohr magneton, approximately 8.5, is larger than the free ion value and thus indicates positive polarization. Similarly, Nelson observes a Curie constant and therefore effective Bohr magneton larger than the free ion value. His value was obtained for the case of 0.3 atomic percent Gd dissolved in Yttrium, Y. (Reference to a table of electronic configuration of the elements shows that La and Y are very similar.)

The object of this investigation is to study the polarization of conduction electrons by magnetic ions dissolved in the host lattice and to investigate some details of the coupling between these ions. As introduced above the alloy system chosen consists of two members of the rare earths, La and Gd. This group of elements generally has three valence electrons, two in the 6s state and one in the 5d state. The magnetic properties of the rare earths arise from the electrons in the 4f shell. As one proceeds across the periodic table from La to Lu, the 4f shell is progressively filled while the valence band changes very little. La, the host for this study, has no 4f electrons and only a small paramagnetic susceptibility. Gd, the impurity, has seven 4f electrons in a $^8S_{7/2}$ state.

Pure La has been the object of previous investigations. Spedding et al. (26) find its susceptibility to be $+9.83 \times 10^{-6}$, and Berman et al. (3) find γ , the electron specific heat, to be 10.0 millijoule/mole-deg². For their measurements the samples were a mixture of h.c.p. and f.c.c. La. Thus the values may reflect an average of the true values for each phase.

In contrast, specific heat measurement (8) on the samples used in this experiment showed them to be at least 90% h.c.p.

Gd has also been investigated previously and many of its physical properties are known. Nigh (18) has measured the magnetic properties and electrical resistivity of Gd single crystals, and Spedding et al. (26) have measured such things as density (7.868 gm/cm^3), lattice constants for the h.c.p. structure ($a_0 = 3.6360$, $c_0 = 5.7826$), and ferromagnetic Curie temperature (289°K). Gd was chosen because it has a large range of solubility in La, because the valence band contribution is similar to that of La, and because the magnetic moment is spin only. This latter property allows a simpler analysis of many of Gd's interactions. (See, for example, Stoner (28) and van Vleck (33).) Presented here are susceptibility measurements on dilute solutions of Gd in La in the 1 to 20°K range.

II. SAMPLES

The samples used in this experiment are La-Gd alloys. Since their preparation has been described elsewhere (8, 15), only a brief account will be given here. First, La and Gd are arc melted, stirred, and allowed to cool. This procedure is repeated eight times to attain homogeneity. Upon cooling the last time, they are placed in individual tantalum containers, heated for 16 hours at 400°C , and then quickly quenched in water. The 0.2 -, 0.3 -, 0.6 -, and 0.8 atomic percent Gd samples were then used in specific heat experiments (8) and upon completion were stored under vacuum. Approximately six months later they were removed and freshly electropolished for use in this experiment. The last two samples used in this experiment, 1.0 and 1.2 atomic percent Gd, were freshly prepared. No difference in behavior between the two groups was observed.

III. APPARATUS

The experimental phase of this work consists in the measurement of isothermal magnetization curves for the La-Gd alloys. A single magnetometer was designed for use in both temperature ranges of 20°K to 14°K and 4.2°K to 1.8°K .

The procedure used to measure the magnetization curves is similar to that described by Schoenberg (25). The sample is pulled out of the top half of two oppositely wound pick-up coils and the induced current which results is observed as a deflection on a ballistic galvanometer. Since the sample is almost three inches long, the more usual technique of lifting it from the lower to the upper pick-up coil had to be abandoned. For this experiment a Leeds and Nothrup ballistic galvanometer, model 2285-X, with a sensitivity at two meters of $0.00024_{\mu}\text{ coul/mm}$, a CRDX of 960 ohms, and a period of 11.2 seconds is used. As each ballistic deflection is proportional to the sample's magnetic moment (25), a magnetization curve is mapped out at a particular temperature if these deflections are recorded as a function of applied field (29).

A. Temperature Control and Measurement

Isothermal conditions in both the liquid helium and liquid hydrogen temperature ranges are obtained by pumping on the bath. Regulation of the vapor pressure is obtained by a specially designed manostat (14) which is illustrated in Figure 2 and described in detail elsewhere (29). To measure the pressure a $1/4$ inch diameter stainless steel tube that extends to a mean distance of 9 inches above the liquid is used. The absolute temperature is then obtained from the vapor pressure by

TEMPERATURE CONTROL MANOSTAT

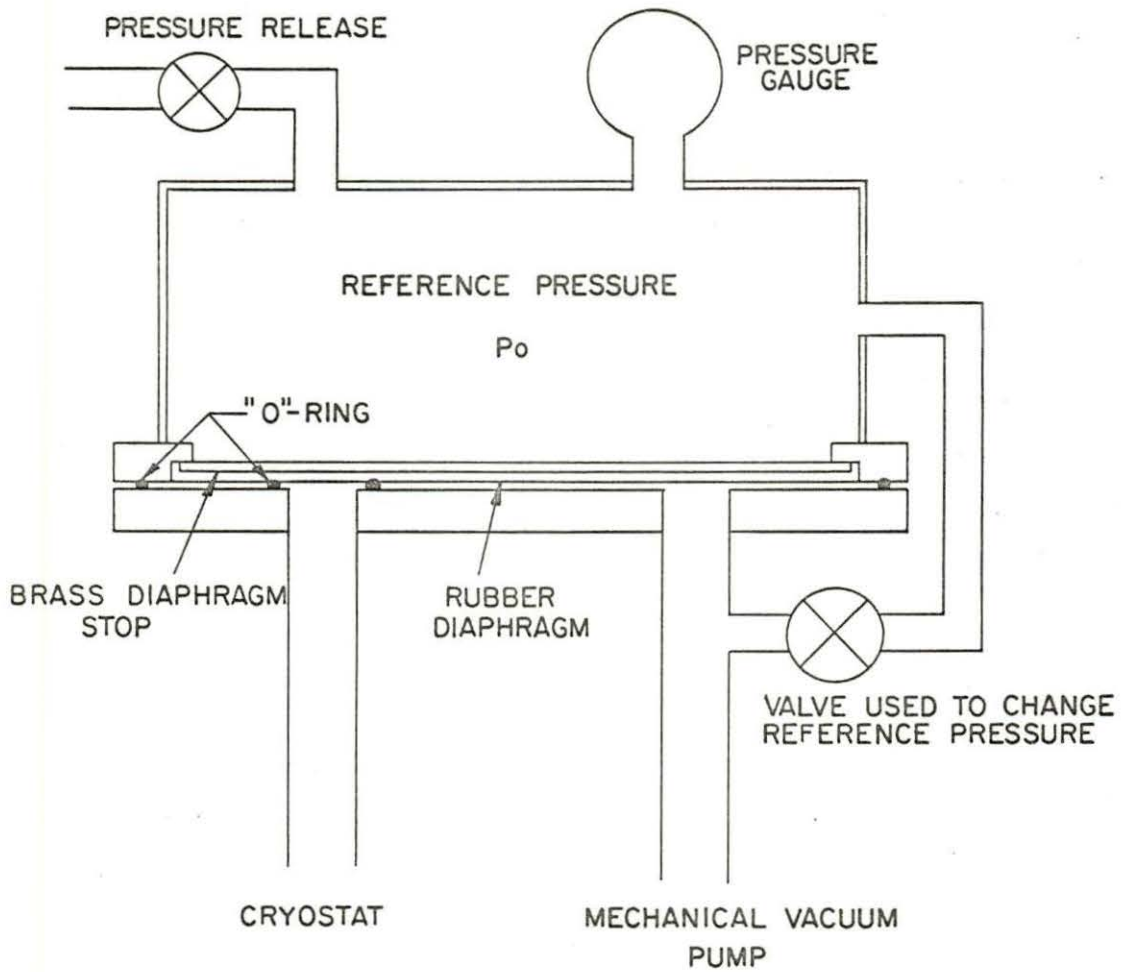


Figure 2. Temperature control manostat

reference to the T_{58} scale (5) for He or the NBS scale for hydrogen (10).

A conventional dewar system, shown in Figure 3, is used. It consists of an outer vacuum jacket, a liquid nitrogen region, a second vacuum jacket, and the liquid helium (or hydrogen) chamber. The enlarged area in the liquid helium chamber is simply to increase the volume.

B. Magnetometer

A schematic drawing of the magnetometer used for both temperature ranges is shown in Figure 4. The upper and lower sections of the pick-up coil are wound with 4000 and 6000 turns of no. 40 copper wire respectively. Its lower section contains more turns since it sits three inches from the center of the applied field and thus sees a slightly smaller field value. In addition, an external trimming resistor (not shown) is connected in parallel with the lower section and is adjusted to provide exact nulling out of field fluctuations.

The first sample holder used was machined out of high purity copper. However, its motion through the magnetic field produced eddy currents which in turn produced deflections of intolerable size. In view of this, a second sample holder was machined out of phenolic. Two phosphor-bronze springs, which are attached to the sample holder by nylon bolts, are used to hold the samples rigidly in place. This latter design is entirely non-metallic, and so completely eliminates the eddy current problem.

Motion of the sample is accomplished by connecting the sample holder to one end of a 3/16 inch diameter stainless steel tube and a soft iron cylinder to the other end. A d.c. solenoid is then placed around the

DEWAR SYSTEM

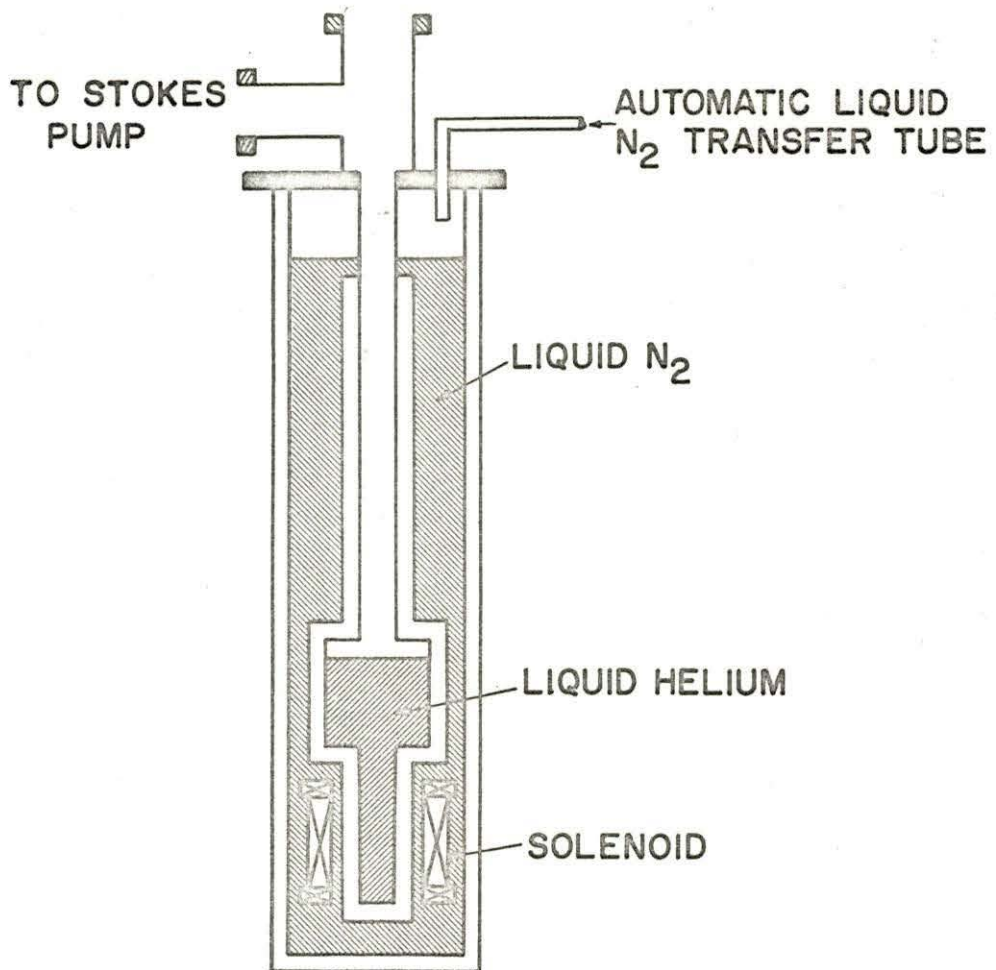


Figure 3. Dewar system

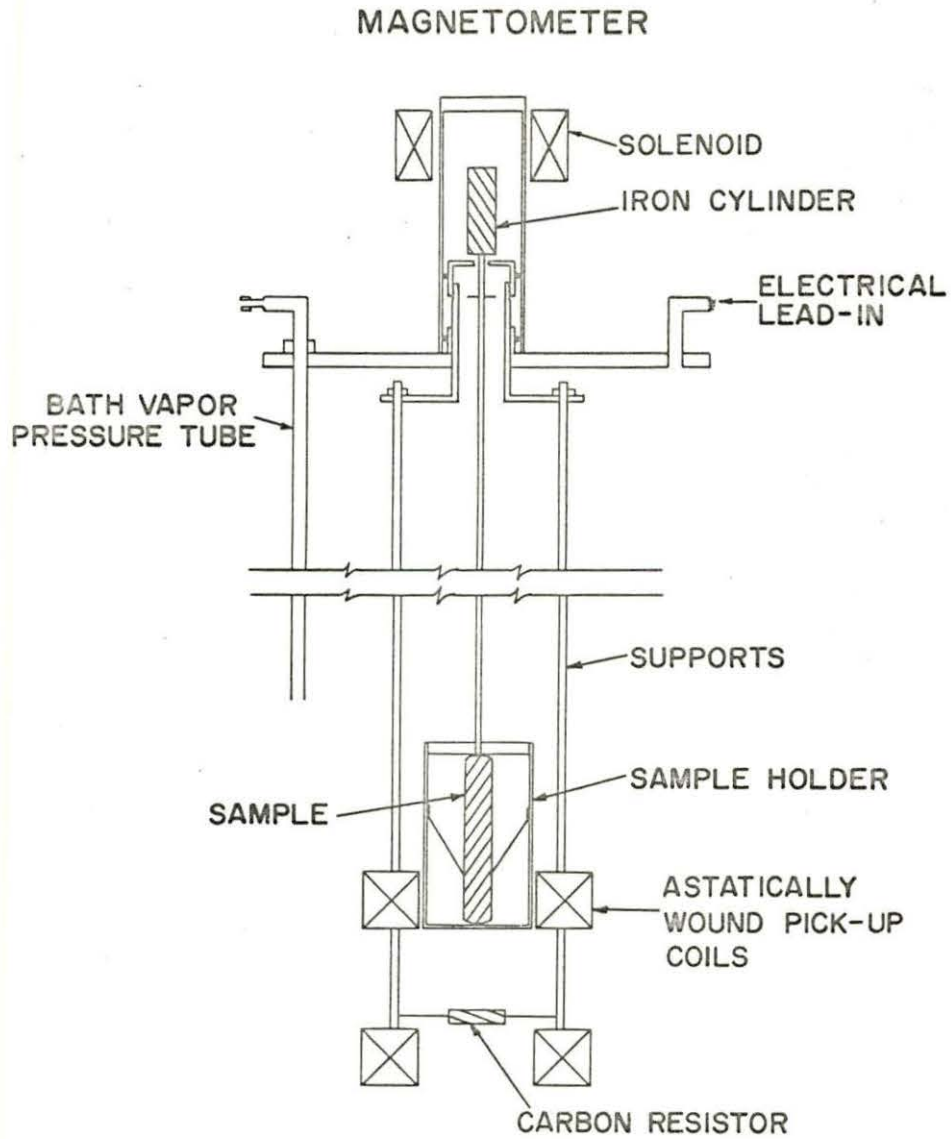


Figure 4. Magnetometer

cylinder. When the circuit is completed the solenoid exerts an upward force on the cylinder and so the sample is lifted. The amplitude of the motion, 1/2 inch, is controlled by stops. When the circuit is broken the sample drops back to its original position. To insure a ballistic effect the time for the motion (less than 1/2 second here) is made small compared to the period of the galvanometer.

C. Magnetic Field

The magnetic field is provided by a liquid nitrogen cooled solenoid with dimensions of 2-1/4 inches I.D. and 8 inches long. Details of its construction and sensitivity are described by Stromberg (29). We note here that the field is uniform to ± 0.01 percent over a distance of 2 centimeters on each side of the center, and that it is continuously variable from 8 to 4400 gauss. The field is measured to the nearest 0.15 or 0.015 gauss depending on whether a 0.10 ohm or 0.01 ohm standard resistor is used to determine the current in the solenoid. Note that measurements are made only on that part of the sample which is in the uniform field region. A schematic circuit diagram is shown in Figure (5).

SCHEMATIC CIRCUIT DIAGRAM

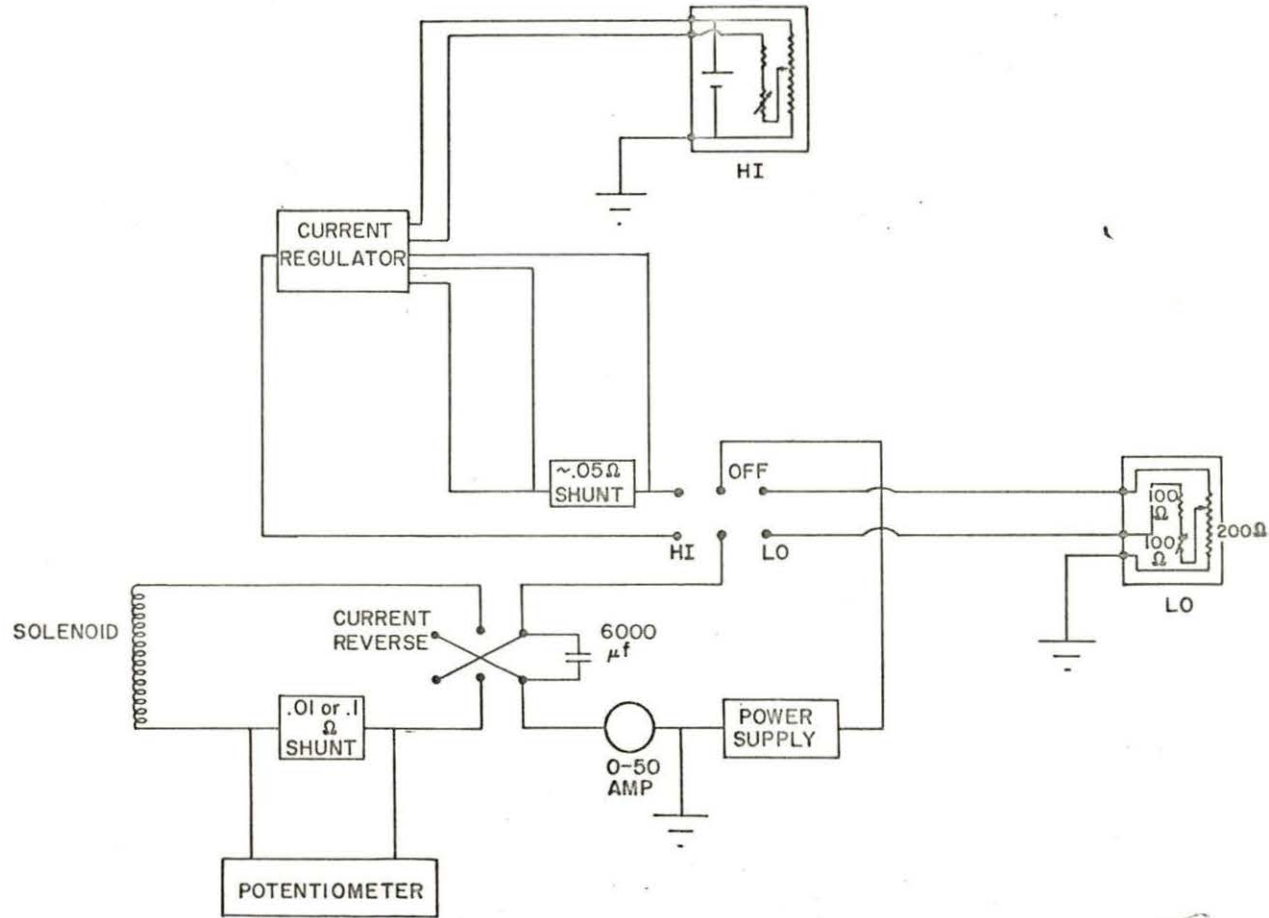


Figure 5. Schematic circuit diagram

IV. CALCULATIONS AND RESULTS

The calculations are made and the results are discussed in terms of the Curie-Weiss theory. For these considerations, the following model of the alloy is used. A random distribution of impurity atoms throughout the host is assumed. The number of impurity atoms per cubic centimeter, N , is given on the average by the reciprocal of the cube root of the concentration. In addition, the host is to provide a background susceptibility and a sea of s-band conduction electrons.

A. Calibration

In order to obtain an absolute value for the magnetization per unit volume, M , and hence the magnetic susceptibility, χ , it is necessary to obtain the proportionality constant between the magnetic moment and the ballistic deflections of the galvanometer. For the data reported here, we have used the susceptibility in the superconducting region where

$$\chi = \frac{M}{H} = - \frac{1}{4\pi} \quad (14)$$

to obtain this proportionality constant. For a given applied field M can be calculated, the corresponding deflection observed and so the proportionality constant is determined. Care has been taken to maintain the resistance of the pick-up coils at a constant value so there is no change in the calibration as the temperature changes.

The shape of the samples used in this work requires a correction for the demagnetizing effects. Here, the sample was approximated as an ellipsoid with length to diameter ratios of 3 to 1 in one direction and

12 to 1 in the other. A geometric mean of the individual demagnetizing factors was then used to approximate the demagnetizing field.

Finally, it is to be noted that a Meissner region was obtained for the 0.2 -, 0.3 -, 0.6 -, and 0.8 atomic percent Gd samples but not for the 1.0 and 1.2 atomic percent Gd samples. For these latter samples, the superconducting critical temperatures were too low (for this and possibly any apparatus) and therefore only relative values for the moments and susceptibilities are reported. The pure La correction to the observed susceptibilities could not be made for these latter two, but the correction is at most 0.6 percent and is thus not important.

B. Calculation of the Susceptibilities and Curie Temperatures

Our primary interest lies in the contribution to the susceptibility by the Gd ions. To separate this quantity from the total observed susceptibility, we assume

$$\chi_{\text{observed}} = \chi_{\text{Gd ions}} + \chi_{\text{La host}} \cdot \quad (15)$$

This assumption is discussed by Shaltiel et al. (24) who show that it is applicable for the rare earths but not in general for other groups. It fails for example in the case of transition elements in Pd due to strong ion-electron interaction. Spedding et al. (26) have measured the susceptibility of La and obtained the value of $+9.83 \times 10^{-6}$ emu. An independent measurement at this laboratory by D. C. Hopkins¹ shows very nearly this

¹Hopkins, Donald, Ames, Iowa. Discussion of the susceptibility of La. Private communication. 1965.

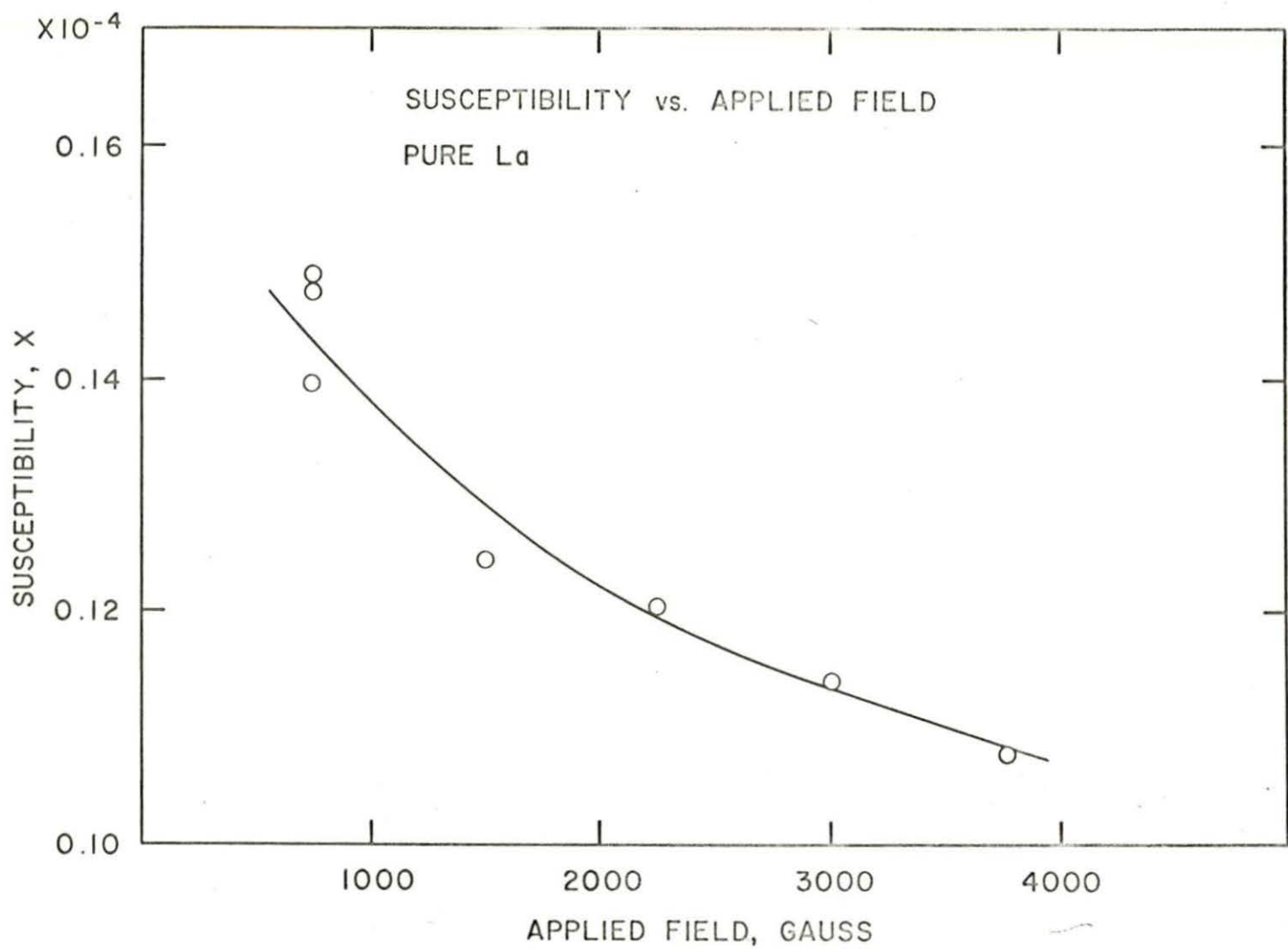


Figure 6. Susceptibility vs. applied field for pure La

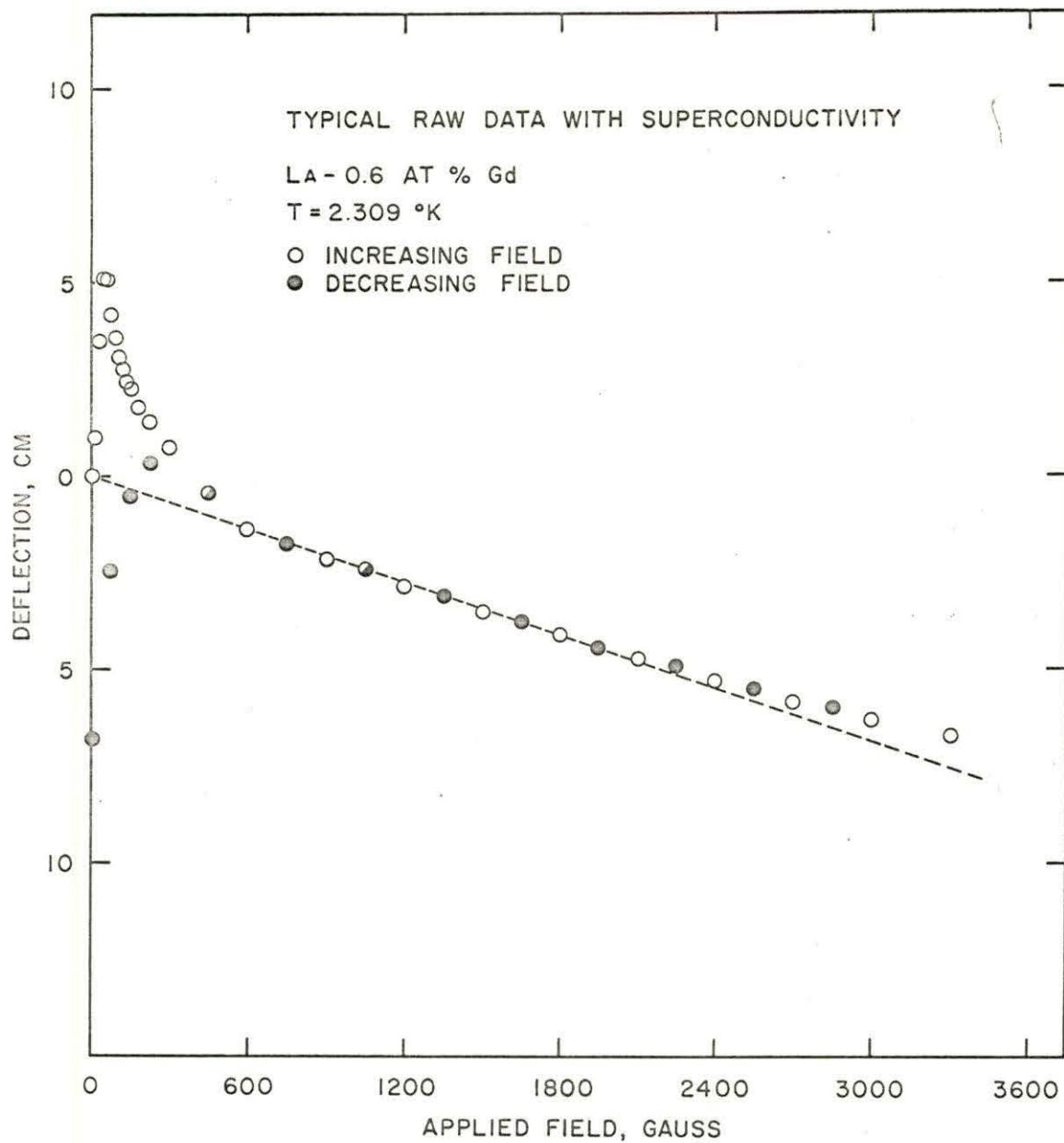


Figure 7. Typical raw data with superconductivity

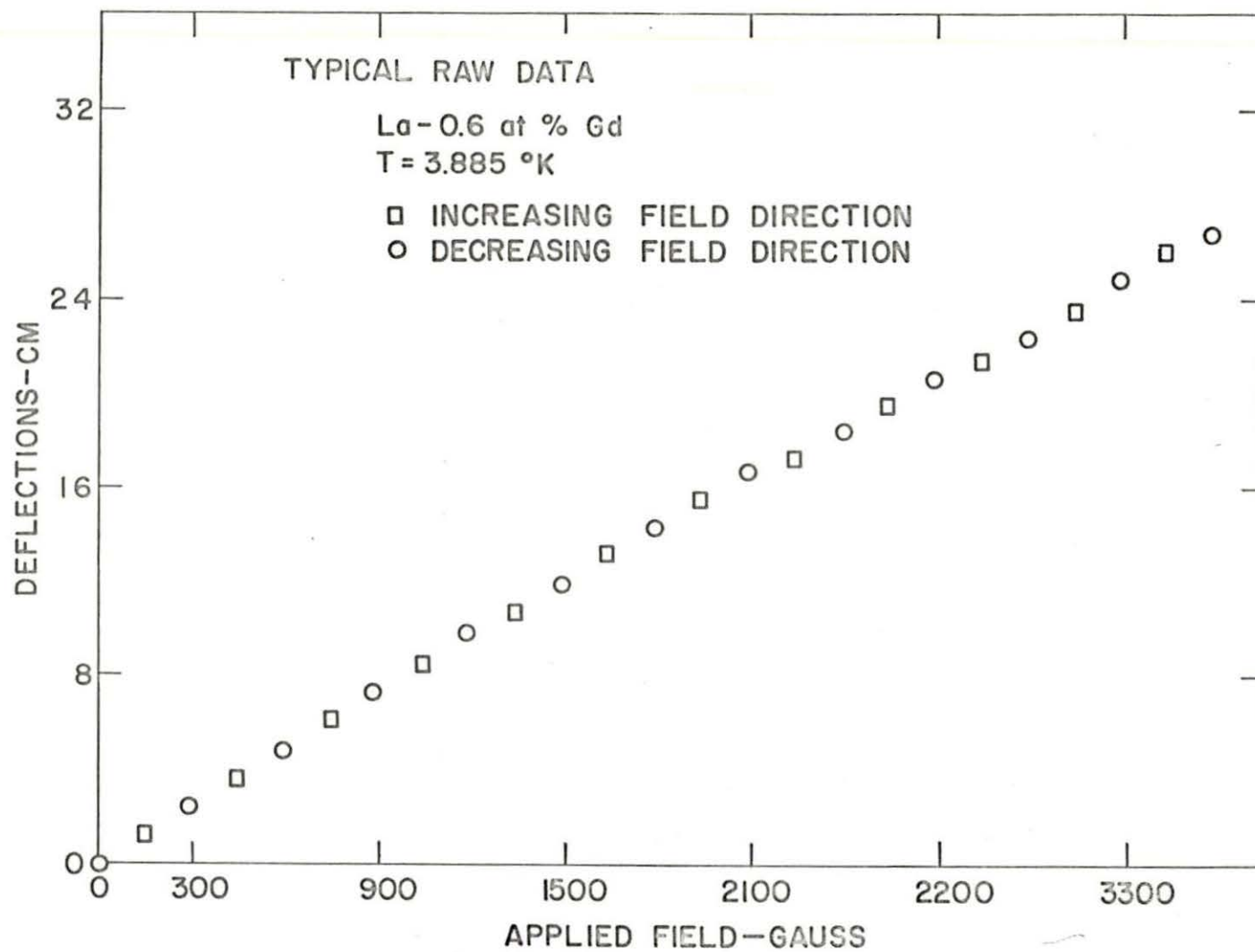


Figure 8. Typical raw data without superconductivity

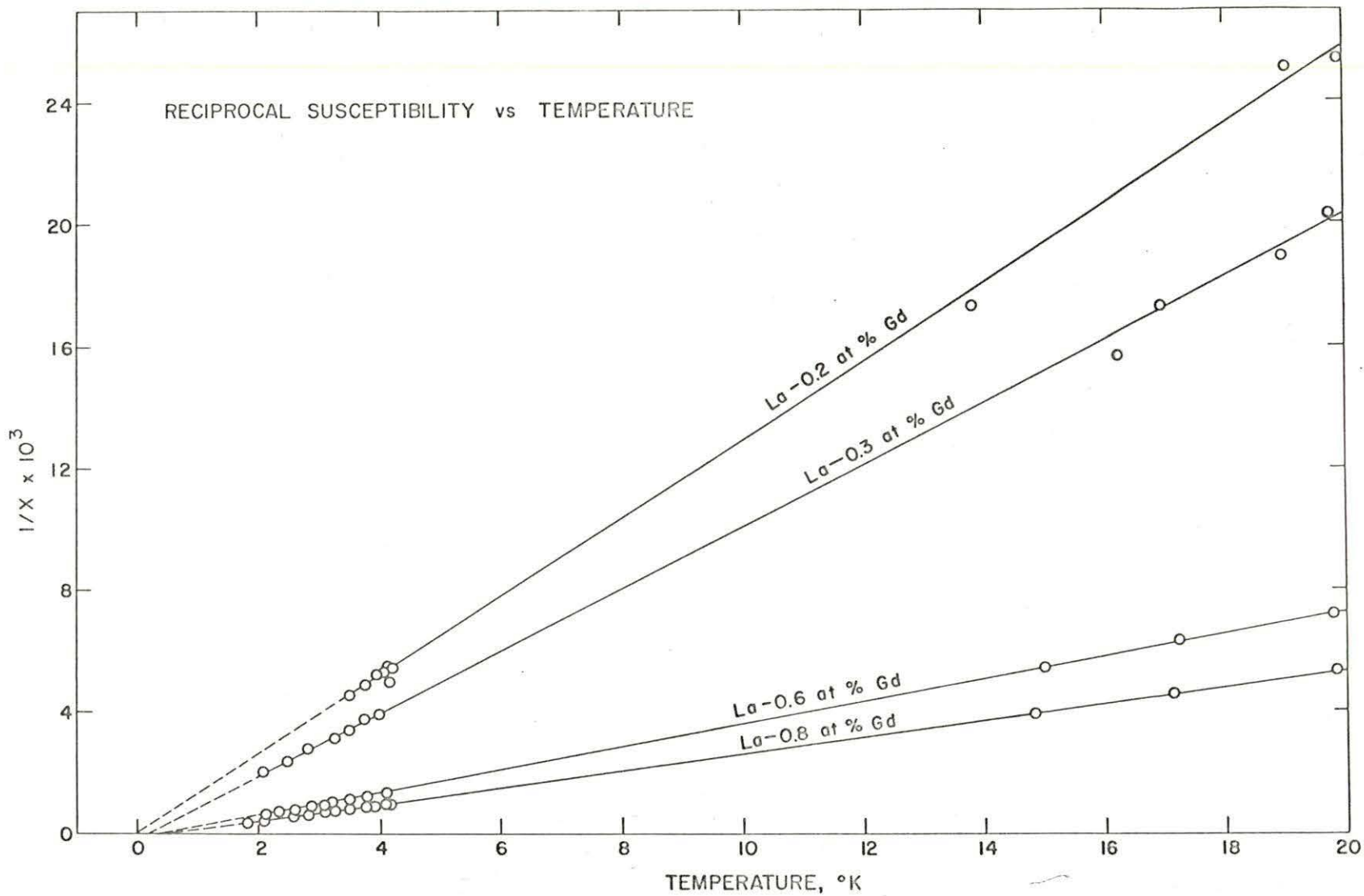


Figure 9. Reciprocal susceptibility vs. temperature for 0.2 -, 0.3 -, 0.6 -, and 0.8 atomic percent Gd

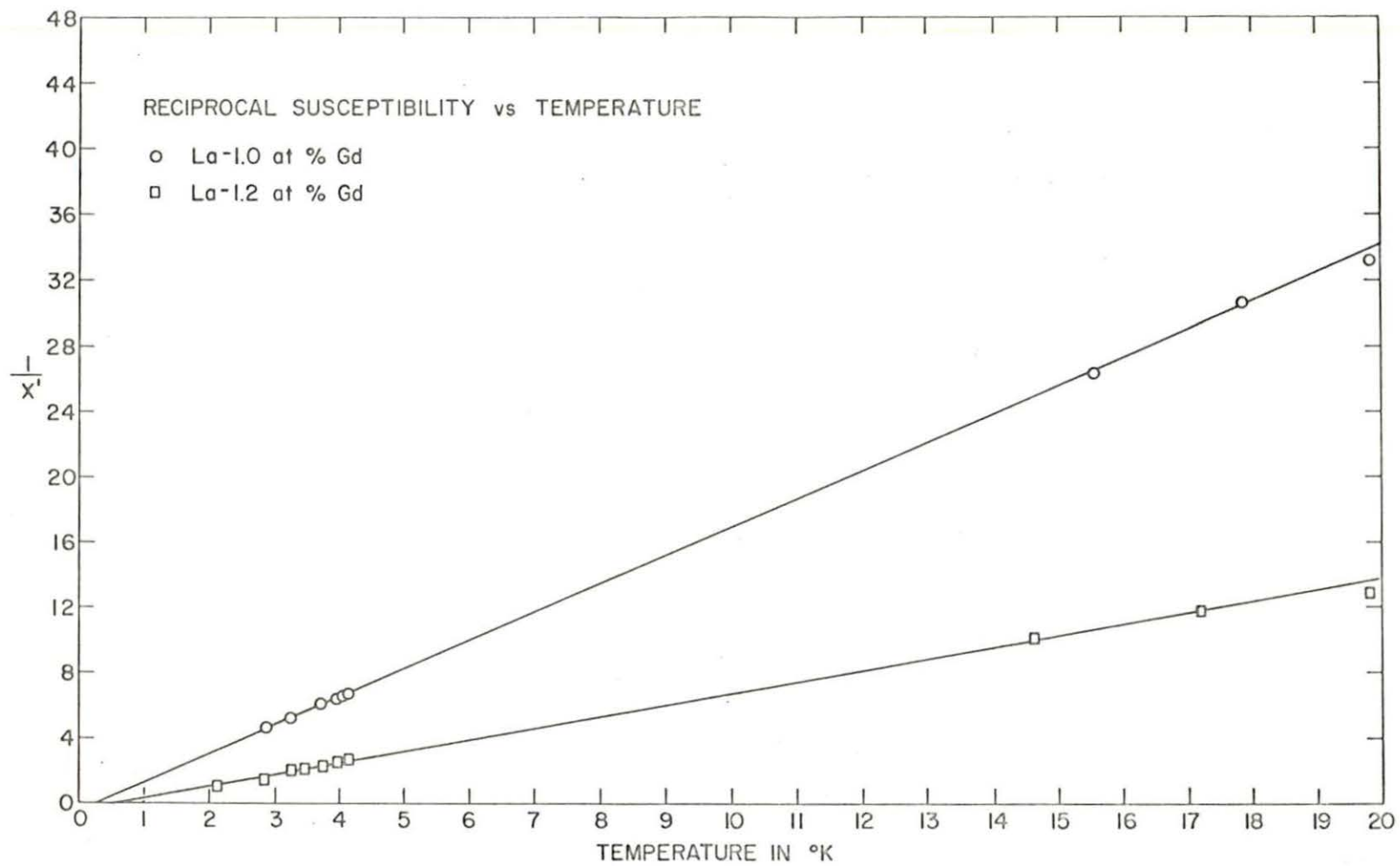


Figure 10. Reciprocal relative susceptibility vs. temperature for 1.0 - and 1.2 atomic percent Gd

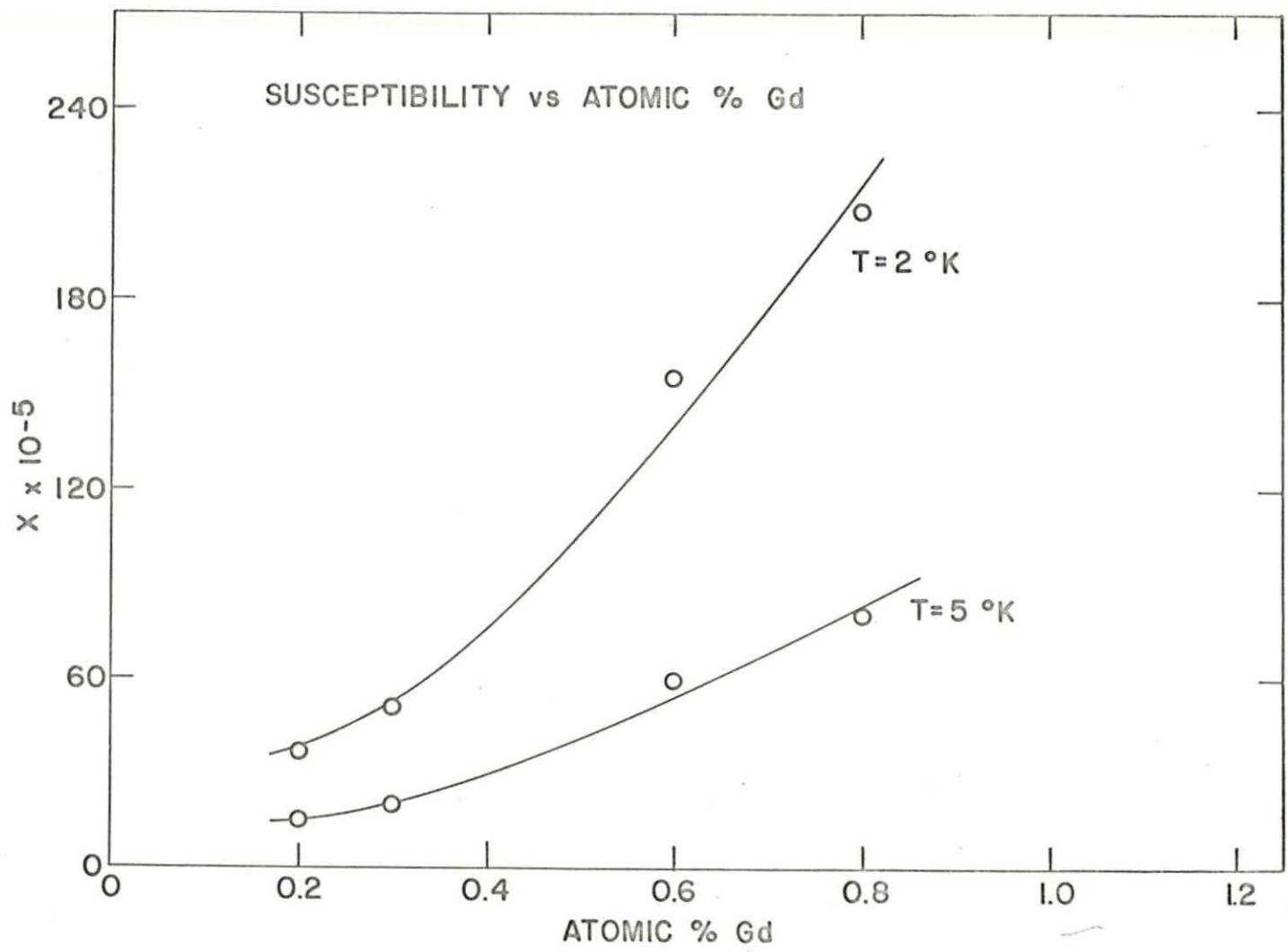


Figure 11. Susceptibility vs. atomic percent Gd for 2 and 5°K

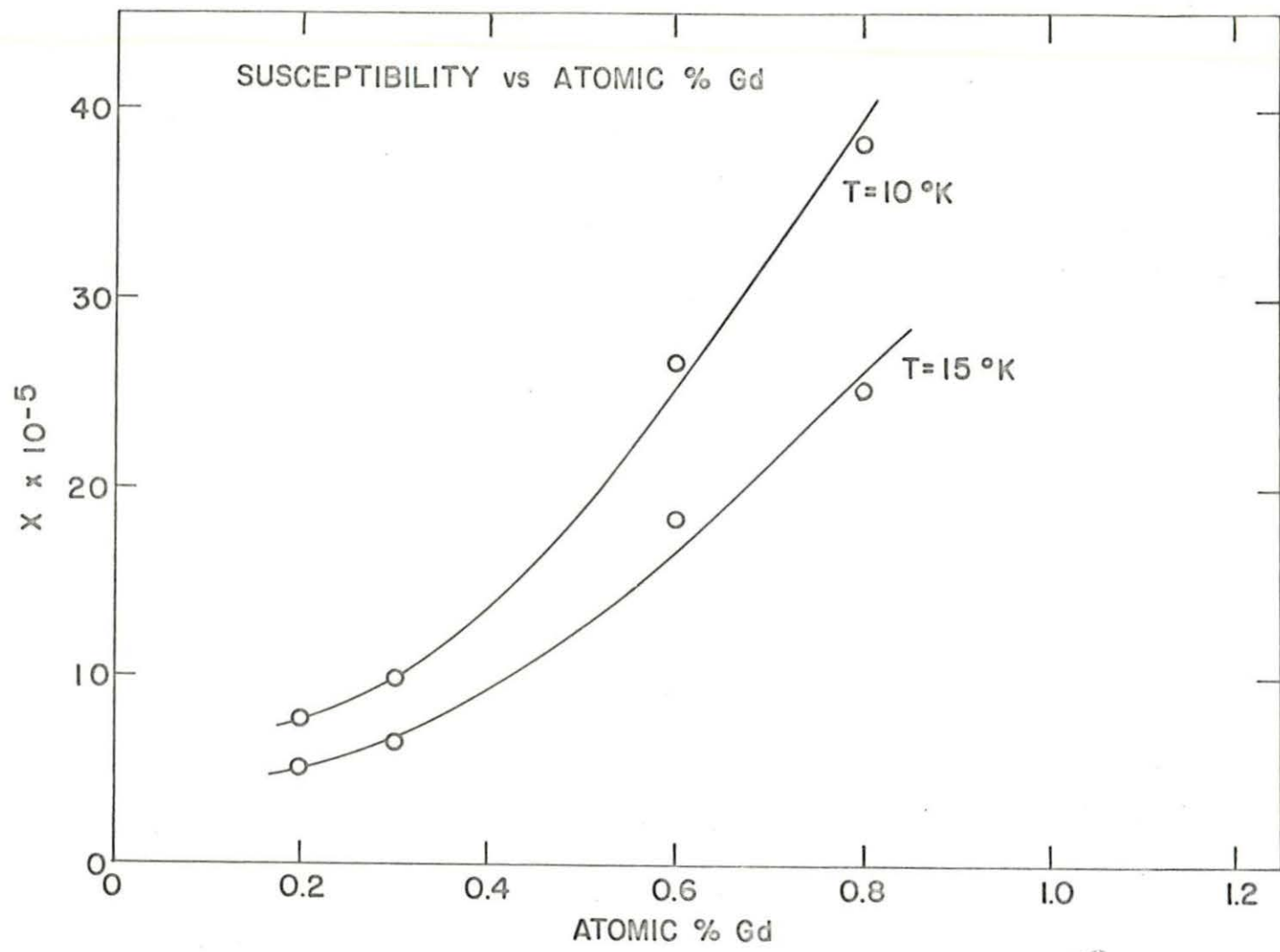


Figure 12. Susceptibility vs. atomic percent Gd for 10 and 15°K

value with a slight dependence on applied magnetic field, see Figure 6. The susceptibility of pure La is thus subtracted from all data and results presented in this work.

Figures 7 and 8 show typical raw data. These are known as magnetization curves and show deflection (proportional to moment) plotted against applied field for constant temperatures. At low fields, the magnetization shows a linear or Meissner region characteristic of superconductivity. The slope in this region is used for calibration. The region from about 40 to 750 gauss shows penetration of flux and quenching of the superconductivity. Purely paramagnetic behavior is shown from 750 gauss on. Note that the paramagnetic region is reversible but that the superconducting region is not. In Figure 8 the magnetization is completely paramagnetic and reversible throughout.

From each isothermal magnetization curve a value of the susceptibility is obtained by measurement of the slope in the low field or linear region. The reciprocal of the susceptibility is then plotted against temperature as shown in Figures 9 and 10. A separate figure is needed for the 1.0 and 1.2 atomic percent Gd samples since only the relative susceptibilities are known here. Notice that these curves are linear over the temperature ranges considered and so can be described by the Curie-Weiss law, Equation 10. It is also of interest to show the variation of susceptibility with Gd content for several temperatures. This is done by choosing the temperatures and reading the reciprocal susceptibilities directly from Figures 9 and 10. The results, shown in Figures 11 and 12, illustrate the expected increase in susceptibility with the increase in Gd content.

The extrapolation used to determine the Curie temperatures is illustrated in Figures 9 and 10. For the actual determination of the Curie temperatures expanded scales are used and the error bars are determined by drawing the two most extreme lines through the data. To display the precision, Figure 13 shows the Curie temperatures with error bars plotted against atomic percent Gd. To show the trend in Curie temperatures more completely Figure 14 combines the results of this experiment with those quoted in Matthias et al. (16). Caution must be used here as the Curie temperatures reported in this work are more correctly known as paramagnetic Curie temperatures since they result from extrapolation of the paramagnetic data. Those quoted in Matthias et al., however, are known as ferromagnetic Curie temperatures and result from ferromagnetic data. These two Curie temperatures are not distinguished between within the Curie-Weiss theory but are observed to be slightly different. The reason for combining the results into Figure 14 is that a similar trend in Curie temperatures with impurity content was observed by Owen et al. (19) for Mn in Cu over the concentration range of 0.03 to 11.1 atomic percent and by Crangle (6) for Gd in Pd over the concentration range of 1.0 to 10 atomic percent.

An antiferromagnetic transition is suggested by the slightly negative value of the Curie temperature for the 0.2 atomic percent Gd sample. In order to pursue this possibility it was decided to construct plots of magnetization, M , against temperature, T , for several values of applied field, H . These are shown in Figures 15 through 20. If an antiferromagnetic transition occurs then these curves should show a characteristic hump or relative maximum. Slight irregularities are observed, especially

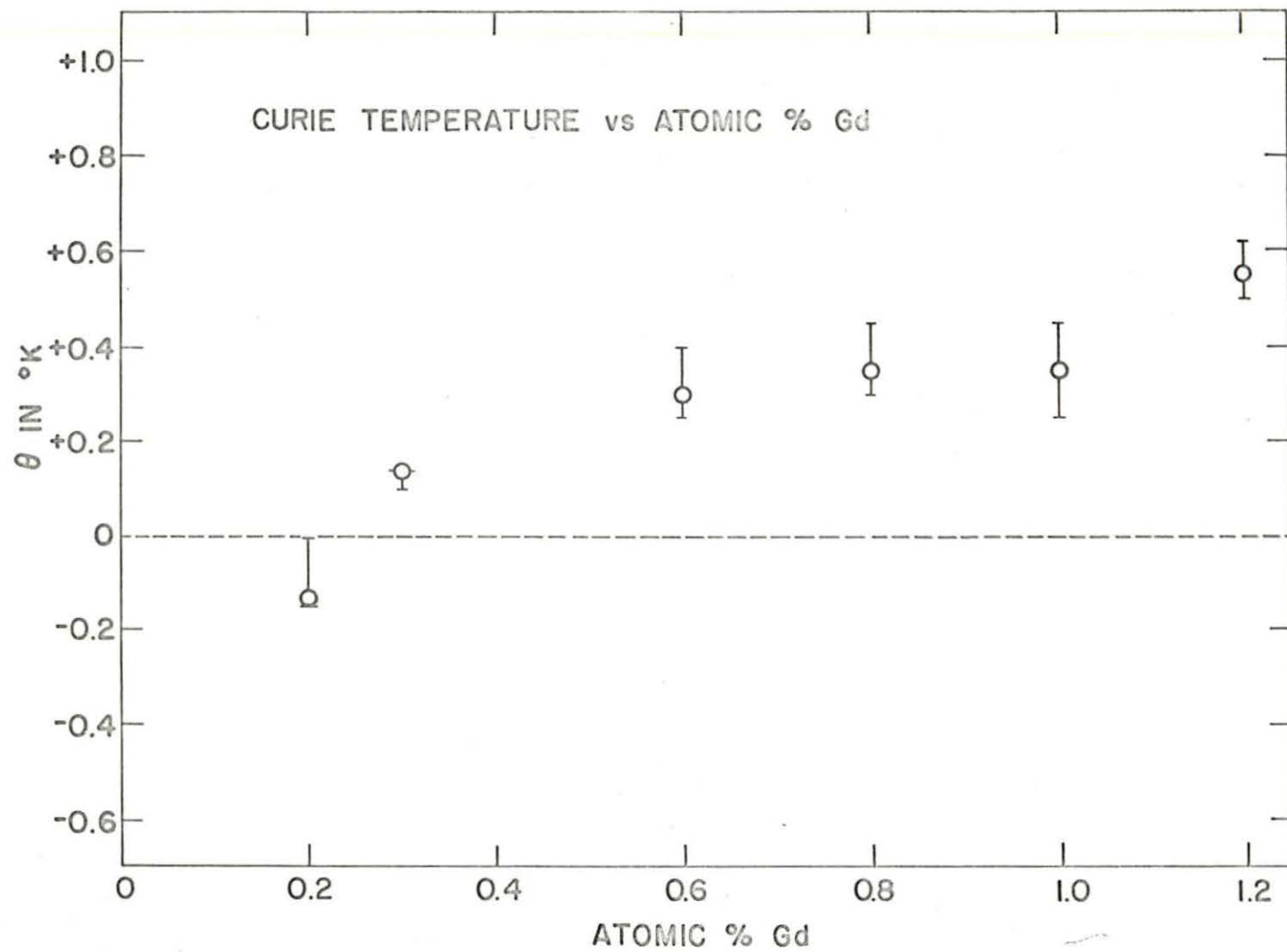


Figure 13. Curie temperature vs. atomic percent Gd

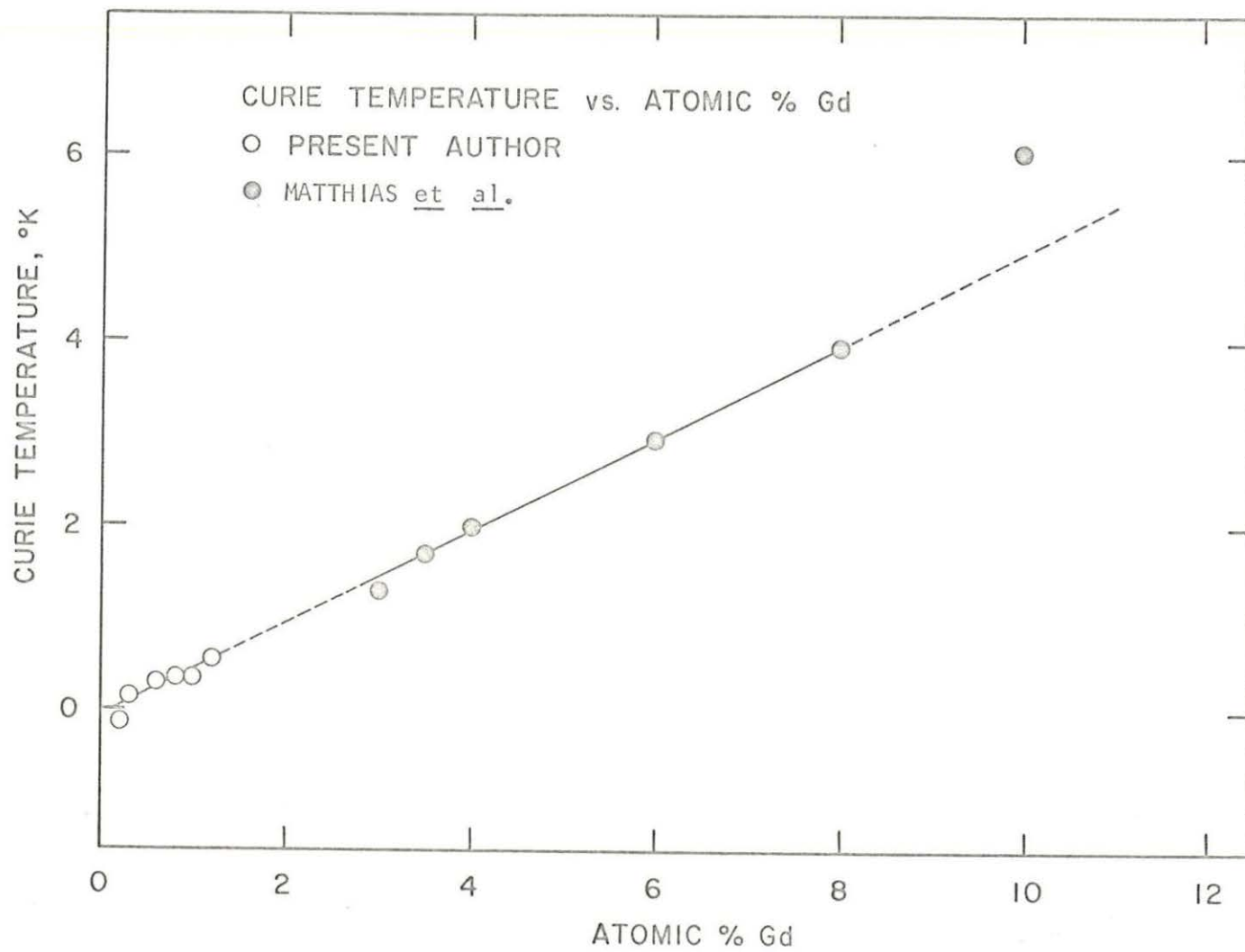


Figure 14. Curie temperature vs. atomic percent Gd, combined results

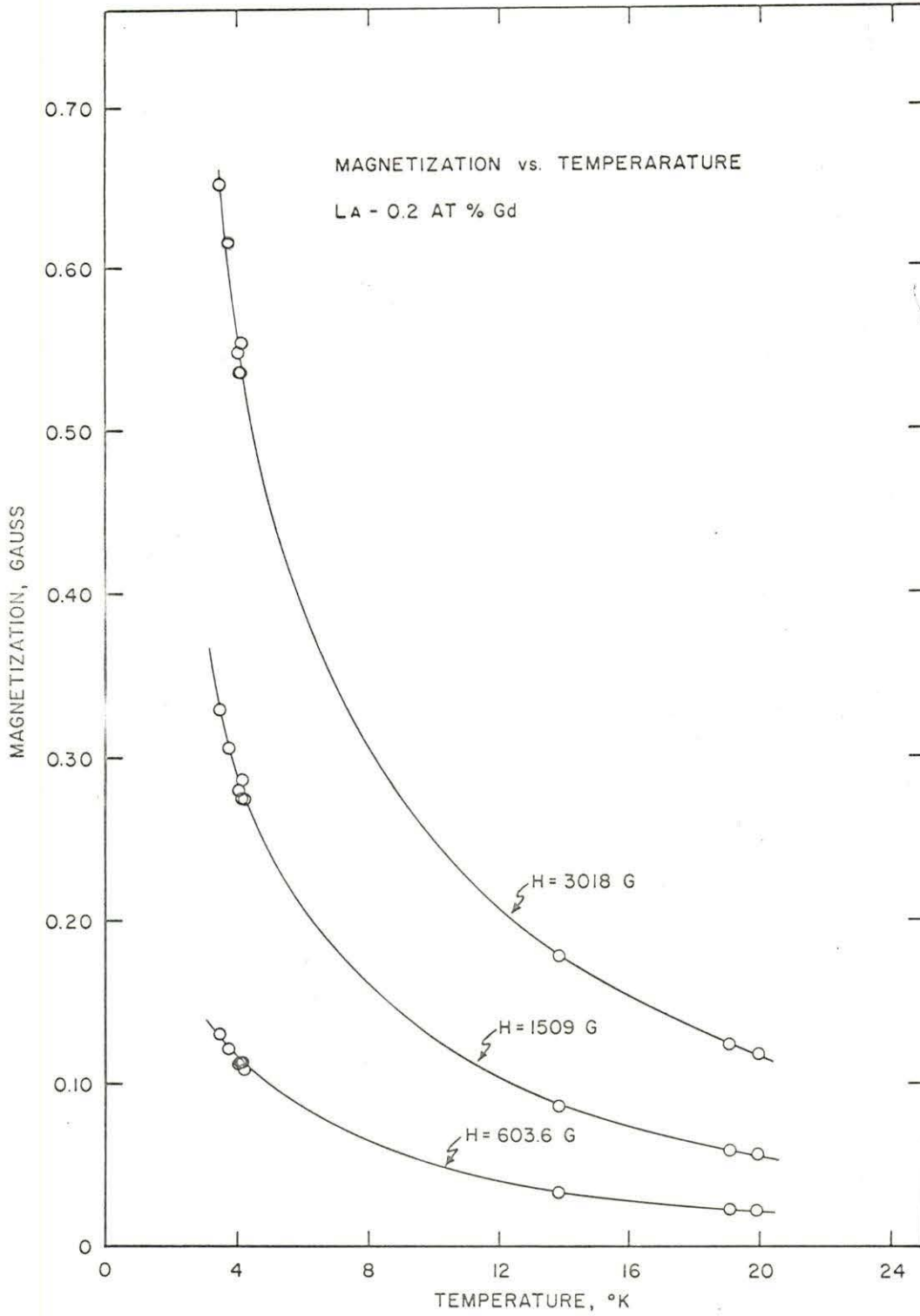


Figure 15. Magnetization vs. temperature at constant fields for 0.2 atomic percent Gd

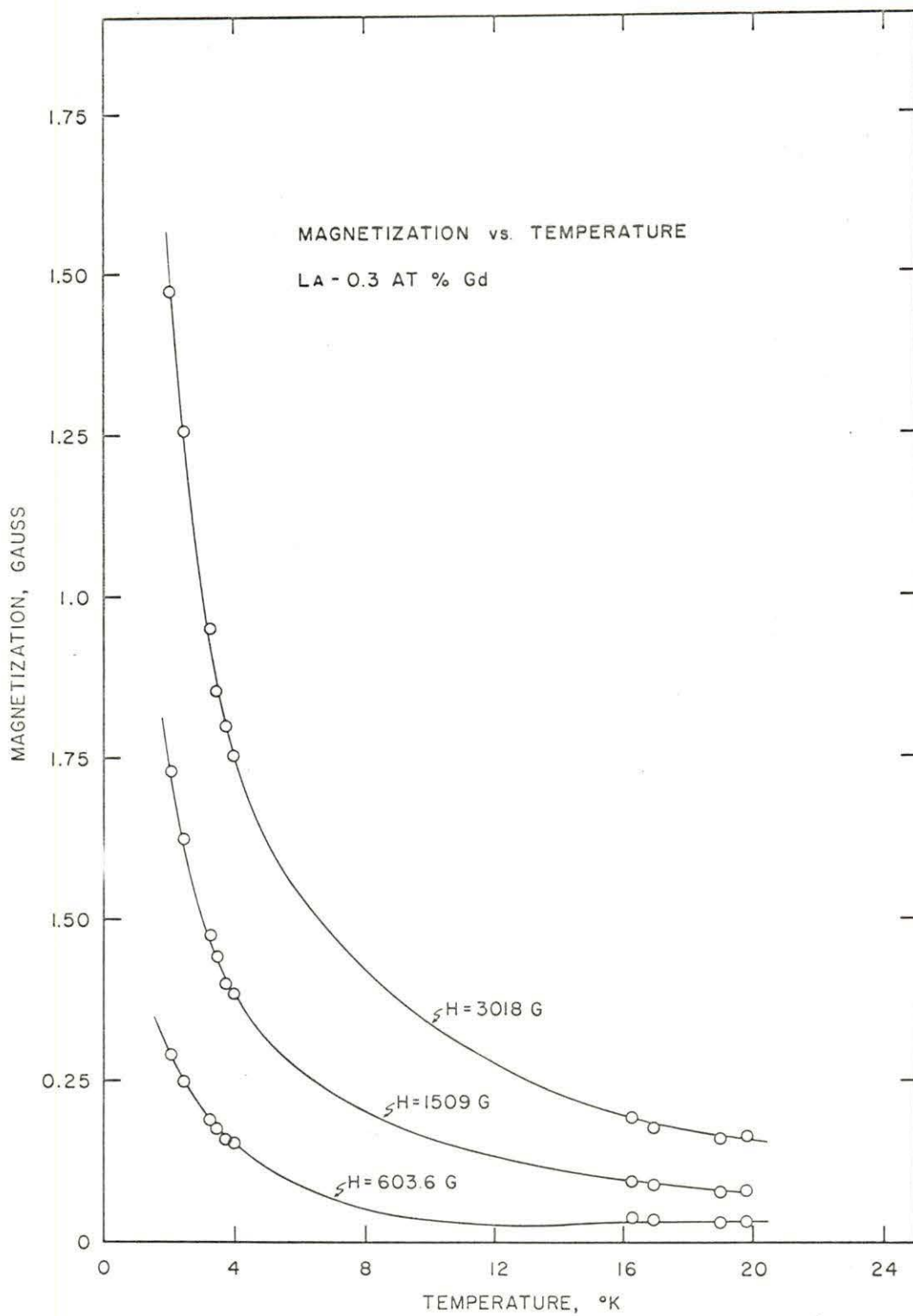


Figure 16. Magnetization vs. temperature at constant fields for 0.3 atomic percent Gd

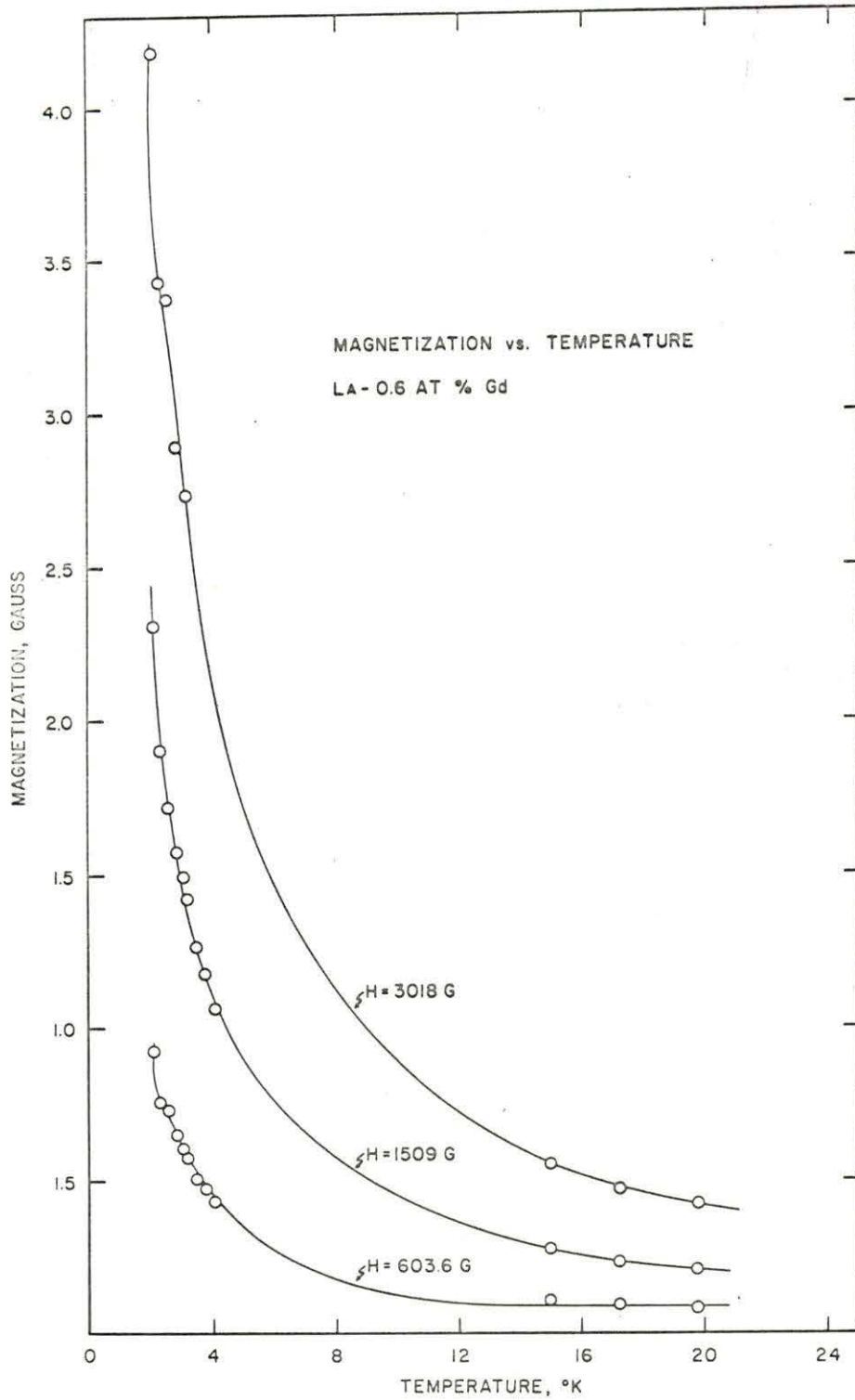


Figure 17. Magnetization vs. temperature at constant fields for 0.6 atomic percent Gd

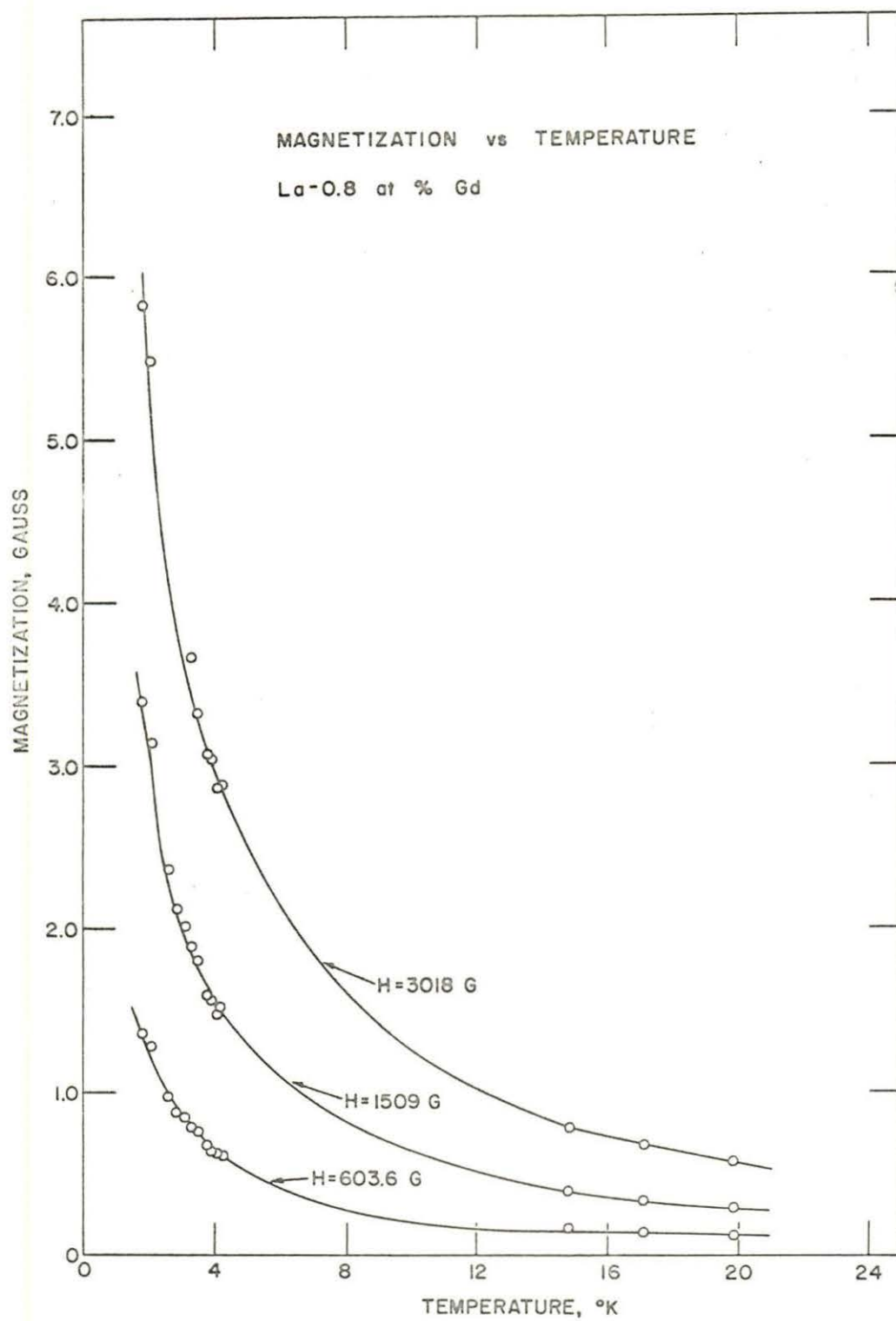


Figure 18. Magnetization vs. temperature at constant fields for 0.8 atomic percent Gd

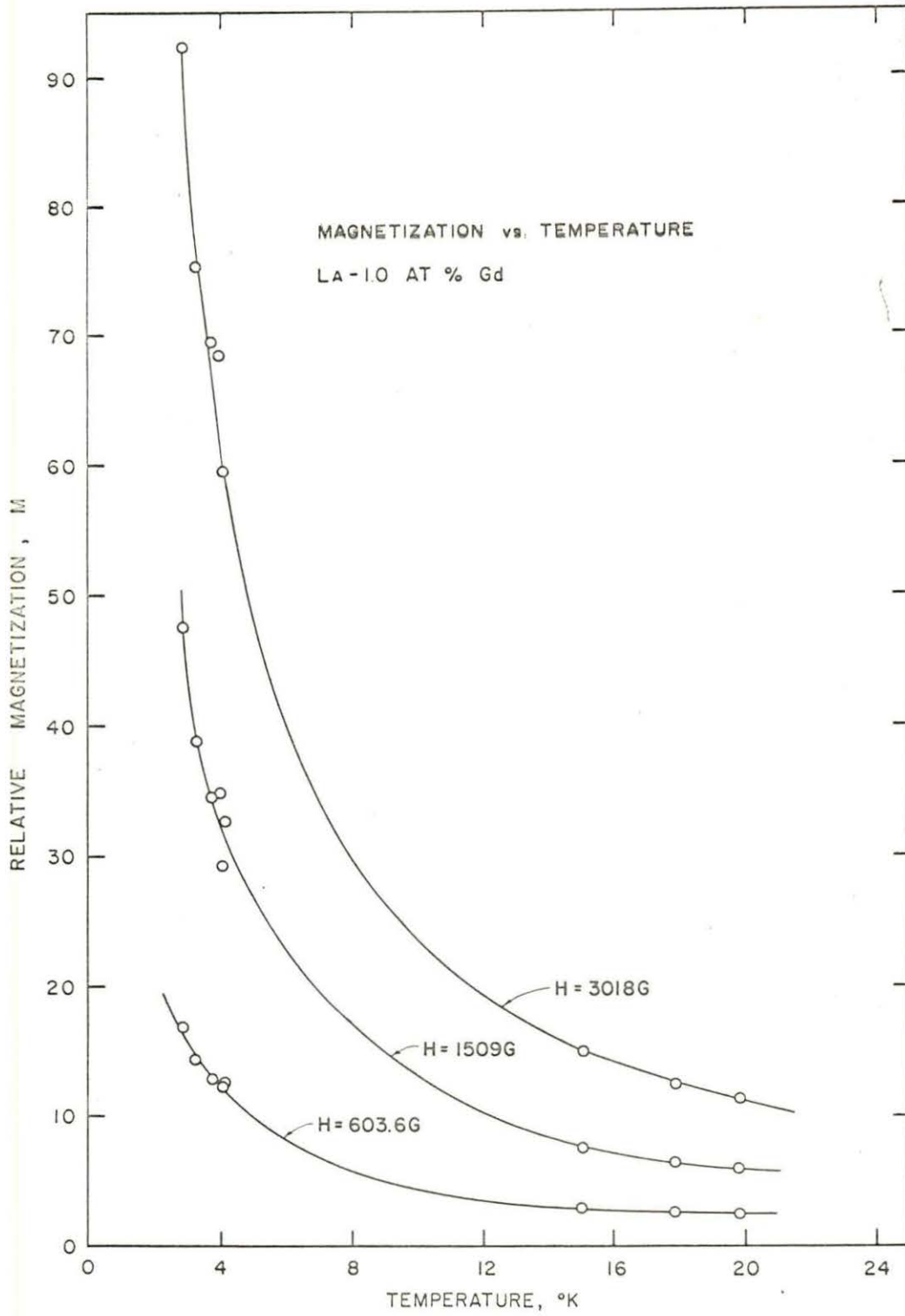


Figure 19. Relative magnetization vs. temperature at constant fields for 1.0 atomic percent Gd

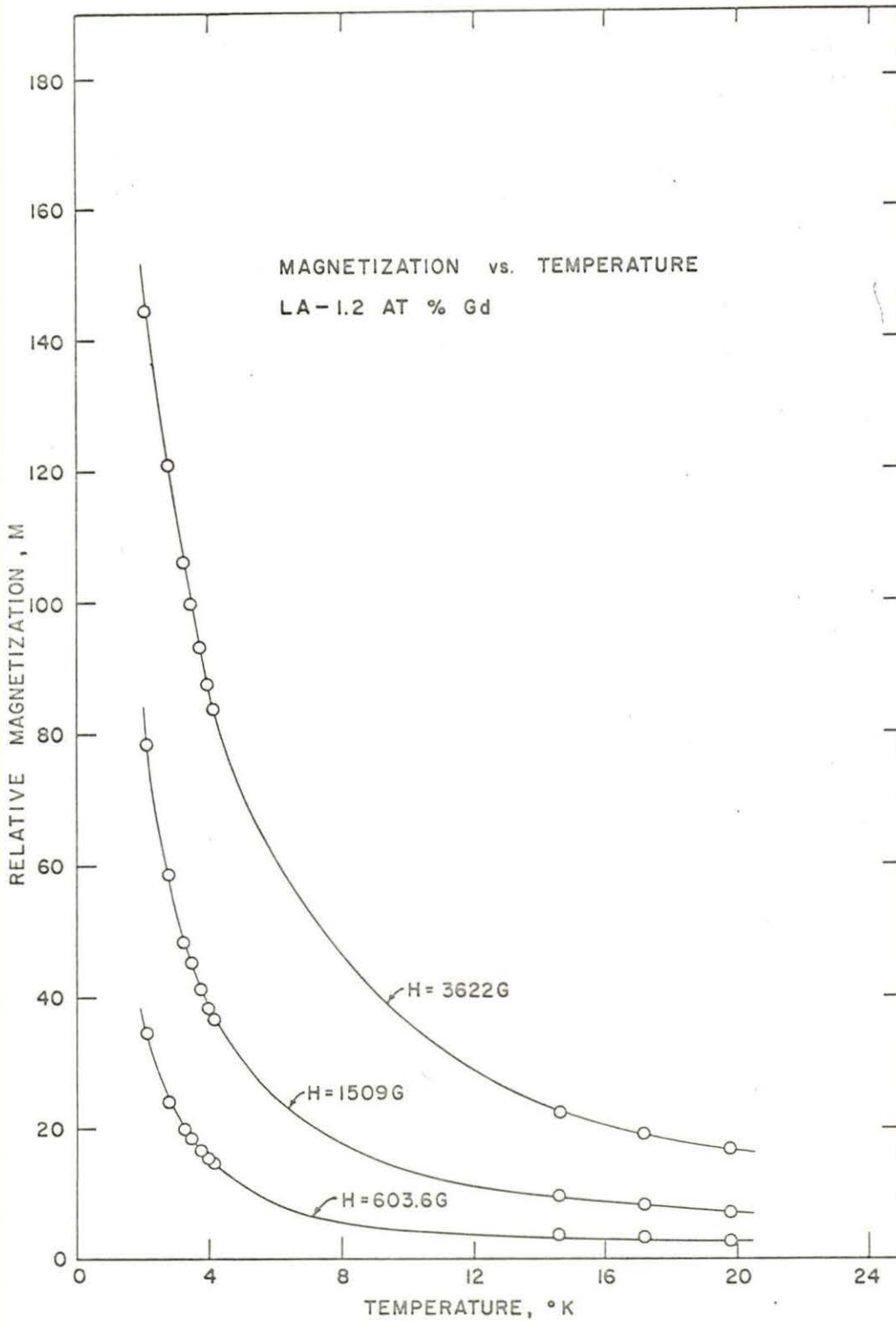


Figure 20. Relative magnetization vs. temperature at constant fields for 1.2 atomic percent Gd

for the 0.8 and 1.0 atomic percent Gd samples, at about 4°K. However, these irregularities are very narrow and the data is insufficiently precise to resolve them. Therefore, an antiferromagnetic transition cannot be definitely established.

C. Calculation of Effective Bohr Magnetons and Curie Constants

Since the 4-f electrons are buried in the Gd core, the magnetic coupling is probably made through the conduction electrons. One measure of the influence of the conduction electrons on the Gd is the shift in the effective moment of the Gd ion from the free value of 7.94 calculated for a $8S_{7/2}$ state. As discussed above, agreement with the free ion value indicates the 4-f electrons are essentially free even in the alloy. A larger value indicates a parallel polarization and, similarly, a smaller value indicates an antiparallel polarization of the conduction electrons. The number of effective Bohr magnetons is calculated from Equation 13

$$P_{\text{eff}} = \left[\frac{3k (T - \theta) \chi}{N\mu_B^2} \right]^{1/2} \quad (13)$$

where k is Boltzmann's constant, T is absolute temperature, χ is the susceptibility, N is the number of Gd ions per cubic centimeter, and μ_B is the Bohr magneton. The values so obtained are listed in Table I. Notice that the observed values of approximately 8.84 are larger than the value for the free Gd $+3$ ion. Within the above discussion this indicates a net positive or parallel polarization of the conduction electrons.

As would be expected, a plot of P_{eff} against temperature for a

particular sample, Figure 21, shows no dependence on temperature. However a plot of P_{eff} against atomic percent Gd, Figure 22, shows a slight tendency for P_{eff} to increase as the Gd content increases. The anomalous result for the 0.3 atomic percent Gd sample is not understood.¹ Note that a similar increase in P_{eff} with impurity content was also observed by Crangle (6) for Gd in Pd.

From the statement of the Curie-Weiss law, Equation 10

$$\chi = \frac{C}{T - \theta} \quad (10)$$

it is evident that the reciprocal of the Curie constant, C , is given by the slope of the temperature-reciprocal susceptibility curves. The observed Curie constants so obtained are listed in Table 1. Notice that they are on the average about 30 percent larger than the values calculated from Equation 8

$$C = \frac{Ng^2 J (J + 1) \mu_B^2}{3k} \quad (8)$$

Nelson (17) makes a similar observation for 0.3 atomic percent Gd in Y, but his observed value for C is almost twice as large as the calculated value.

¹This sample received slightly different treatment before use in this experiment. It was spark-cut into two sections for use in X-ray analysis. While this sample cannot be completely disregarded, the results obtained for it are questioned.

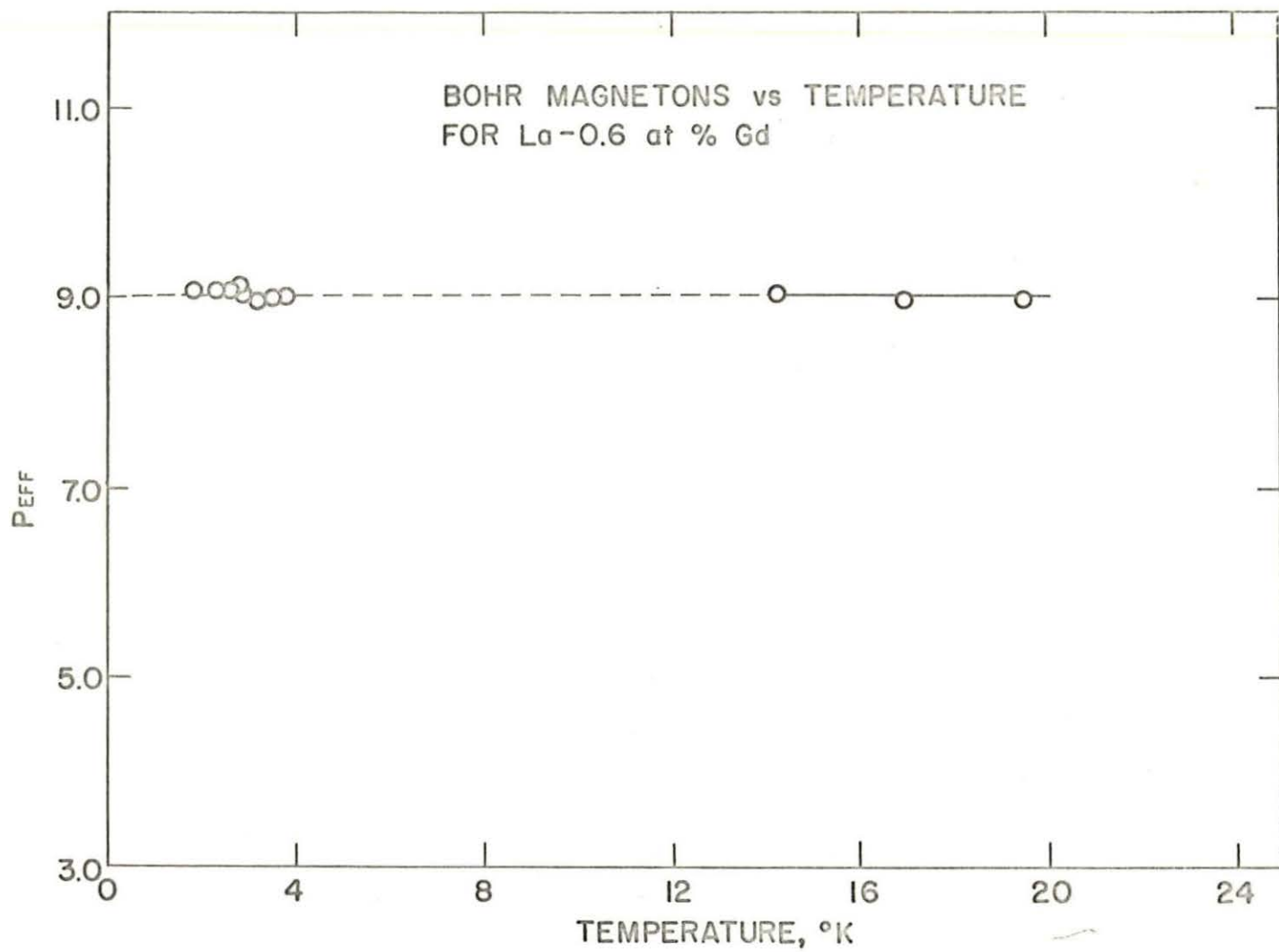


Figure 21. Effective Bohr magnetons vs. temperature for 0.6 atomic percent Gd

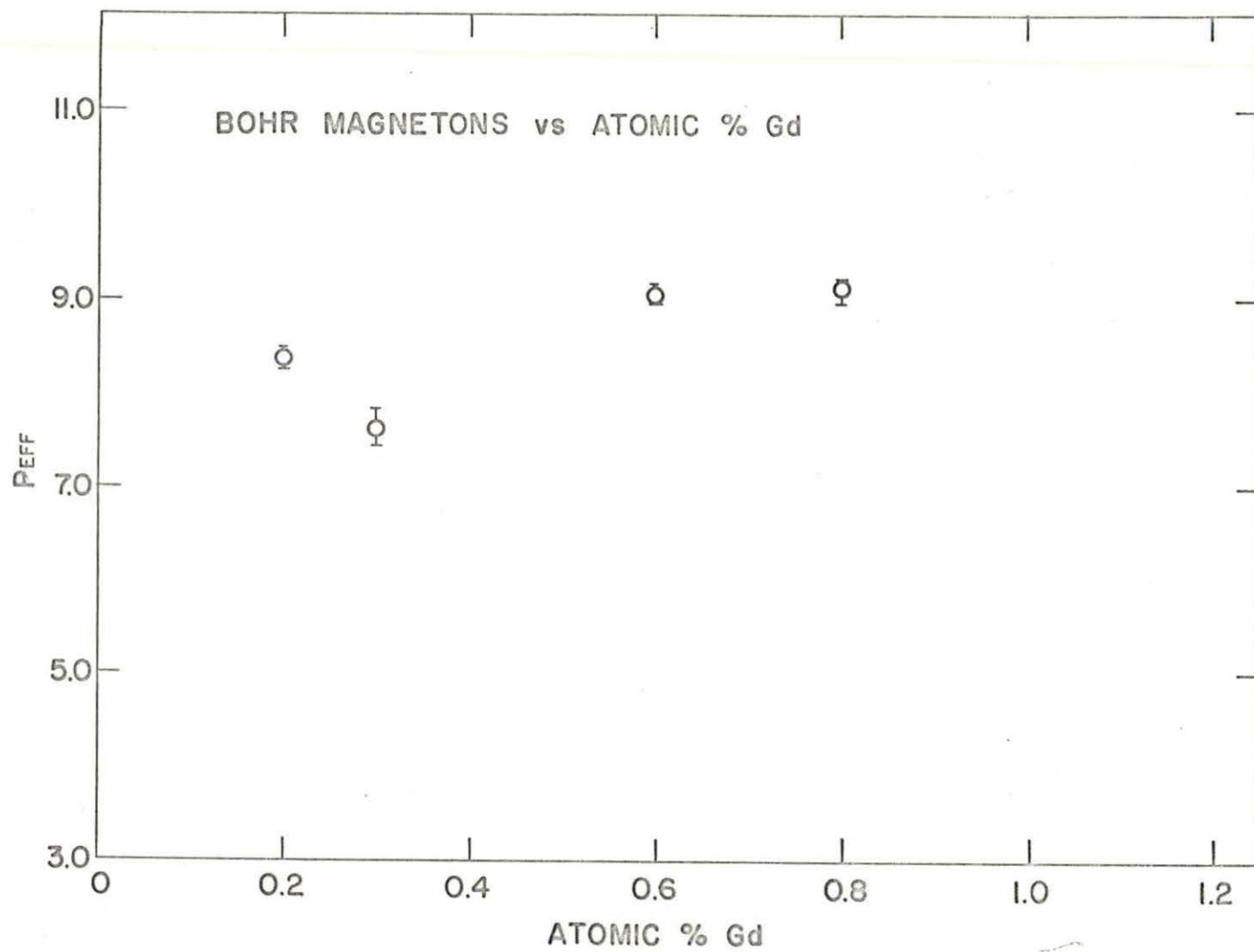


Figure 22. Effective Bohr magnetons vs. atomic percent Gd

Table 1. Summary of Results

Sample	Curie Temperature $\theta, ^\circ\text{K}$	Effective Magnetons P_{eff}	Bohr Weiss Constant λ	Curie Constant Theoretical $C_{\text{theor}}, ^\circ\text{K}$	Curie Constant Observed $C_{\text{obs}}, ^\circ\text{K}$	Weiss Molecular Field Hm, gauss
La - 0.2 at % Gd	+0.02 - 0.13 -0.13	+0.10 8.37 -0.10	- 185	0.000704	0.000770	10 - 4300
La - 0.3 at % Gd	+0.00 0.14 -0.04	+0.22 7.62 -0.17	132	0.00106	0.000982	"
La - 0.6 at % Gd	+0.10 0.30 -0.05	+0.11 9.03 -0.08	142	0.00211	0.00272	"
La - 0.8 at % Gd	+0.10 0.35 -0.05	+0.09 9.11 -0.17	124	0.00282	0.00371	"
La - 1.0 at % Gd	+0.10 0.35 -0.10	--	99	0.00352	--	"
La - 1.2 at % Gd	+0.07 0.55 -0.05	--	130	0.00422	--	"

D. Calculation of the Weiss Constants and Molecular Fields

The final calculations to be made are for the Weiss constants, λ , and the molecular fields, H_m . Equation 11

$$\lambda = \frac{\theta}{C} \quad (11)$$

gives the Weiss constant as the ratio of the Curie temperature to the Curie constant. Since we have experimentally established the Curie temperatures to be roughly proportional to the Gd concentration and since, by theory, the Curie constant is also proportional to the Gd concentration, the Weiss constant is not expected to show any systematic deviation with Gd concentration. This is born out in the calculation. Table 1 lists the results and the mean value for λ is 134. Note that the value of λ obtained here is about 100 times less than a typical value for a ferromagnetic material. This is considered to be reasonable since the concentrations considered are of the order of 1 percent.

Rough estimates of the molecular field, H_m , can also be made. For a typical sample, 0.6 atomic percent Gd, the magnetization can be taken from Figure 17. Since the Weiss constants have been determined above, Equation 9 yields the molecular fields. Table 1 shows the range of values so obtained. The minimum field changes from an original value of 8 gauss to a new value of about 10 gauss. For the maximum field, the original value of about 3600 gauss changes to an estimated value of 4300 gauss.

V. SUMMARY AND CONCLUSION

The susceptibilities of these alloys in low fields obey a Curie-Weiss law over the temperature range of 1.8 to 20°K. Therefore, the number of Bohr magnetons, μ_B , the Curie temperatures, θ , the Weiss constants, λ , the molecular fields, H_m , and the theoretical and observed Curie constants, C_{theor} and C_{obs} have been calculated. For convenience, all these results are summarized in Table 1.

The mean value¹ of the observed number of effective Bohr magnetons is 8.84 which is larger than the theoretical value of 7.94 for the free Gd ⁺³ ion. In terms of the above discussion this indicates a net positive or parallel polarization of the conduction electrons. Similar observations were made by Thoburn (32) on Gd in La and by Nelson (17) on Gd in Y. The slight increase in P_{eff} with Gd concentration may indicate a cooperative aspect to the conduction electron polarization.

In the paramagnetic region we find a tendency toward parallel or ferromagnetic coupling between the Gd ions as evidenced by the generally positive values of the Curie temperatures. If these values of θ are combined with the higher concentration values quoted in Matthias et al. (16) then a roughly linear increase with Gd content is exhibited over the entire concentration range. Similar approximately linear dependence has been observed by Owen et al. (19) for Mn in Cu and by Crangle (6) for Gd in Pd. The slightly negative value of θ for the 0.2 atomic

¹This mean value does not include the anomalous result of the 0.3 atomic percent Gd sample. If included, the mean is 8.53.

percent Gd sample suggested an antiferromagnetic transition but further consideration showed it could not be definitely established.

VI. BIBLIOGRAPHY

1. Anderson, P. W., and Clogston, A. M., Bull. Am. Phys. Soc. 2, 124 (1961).
2. Bates, L. F. Modern magnetism. 1st ed. Cambridge, England, Cambridge University Press. 1939.
3. Berman, A., Zemansky, M. W., Boorse, H. A., Phys. Rev. 109, 70 (1958).
4. Brillouin, L. J., Phys. et. Radium 8, 74 (1927).
5. Brinkwedde, F. G., van Dijk, H., Durieux, M., Clement, J. R., and Logan, J. K., J. Res. Nat. Bur. Stand. 64A, 1 (1960).
6. Crangle, J., Phys. Rev. Letters 13, 569 (1964).
7. Dekker, A. J. Solid state physics. Englewood Cliffs, New Jersey, Prentice-Hall, Inc. 1957.
8. Finnemore, D. K., Johnson, D. L., Ostenson, J. E., Spedding, F. H., and Beaudry, B. J., Phys. Rev. 137, 2A, A550 (1965).
9. Giovanni, B., Peter, M., and Schreiffner, J. R., Phys. Rev. Letters 12, 736 (1964).
10. Hilsenrath, J., Beckett, C., Benedict, W., Fano, L., Masi, J., Luttall, R., Touloukian, Y., and Woolley, H. Tables of thermodynamic and transport properties of air, argon, carbon dioxide, carbon monoxide, hydrogen, nitrogen, oxygen, and steam. New York, New York, Pergamon Press, Inc. 1960.
11. Jaccarino, V., Matthias, B. T., Peter, M., Shul, H., and Wernick, J. H., Phys. Rev. Letters 5, 251 (1960).
12. Kittel, C. Introduction to solid state physics. 2nd ed. New York, John Wiley and Sons, Inc. 1956.
13. Kodie, S., and Peter, M., Rev. Mod. Phys. 36, 160 (1964).
14. Kreitman, M. M., Rev. Sci. Inst. 35, 749 (1964).
15. Leslie, J. D., Capelletti, R. L., Ginsberg, D. M., Finnemore, D. K., Spedding, F. H., and Beaudry, B. J., Phys. Rev. 134, A309 (1964).
16. Matthias, B. T., Shul, H., and Corenzwit, E., Phys. Rev. Letters 1, 92 (1958).

17. Nelson, D. T., Use of metal alloys for adiabatic demagnetization. Unpublished Ph.D. thesis. Ames, Iowa, Library, Iowa State University of Science and Technology. 1960.
18. Nigh, H. E. Magnetization and electrical resistivity of Gadolinium single crystals. Unpublished Ph.D. thesis. Ames, Iowa, Library, Iowa State University of Science and Technology. 1963.
19. Owen, J., Browne, M. E., Arp, V., and Kip, A. F., J. Phys. Chem. Solids 2, 85 (1956).
20. Owen, J., Browne, M. E., Knight, W. D., and Kittel, C., Phys. Rev. 102, 1501 (1956).
21. Peter, M., Shaltiel, D., Wernick, J. H., Williams, H. J., Mock, J. B., and Sherwood, R. C., Phys. Rev. 126, 1395 (1962).
22. Peter, M., Shaltiel, D., Wernick, J. H., Williams, H. J., Mock, J. B., and Sherwood, R. C., Phys. Rev. Letters 9, 50 (1962).
23. Sato, H., Arrott, A., and Kikuchi, R., J. Phys. Chem. Solids 10, 19 (1959).
24. Shaltiel, D., Wernick, J. H., Williams, H. J., and Peter, M., Phys. Rev. 135, A1346 (1964).
25. Shoenberg, D. Superconductivity. 2nd ed. Cambridge, England, Cambridge University Press. 1962.
26. Spedding, F. H., Legvold, S., Daane, A. H., and Jennings, L. D. In Gorter, C. J., ed. Progress in low temperature physics. Vol. 2. p. 368. New York, New York, Interscience Publishers, Inc. 1957.
27. Stoner, E. C., Proc. Leeds Phil. Soc. 3, 457 (1938).
28. Stoner, E. C. Magnetism. 4th ed. London, England, Methuen and Co. Ltd. 1948.
29. Stromberg, T. F. The superconducting properties of high purity niobium. Unpublished Ph.D. thesis. Ames, Iowa, Library, Iowa State University of Science and Technology. 1965.
30. Sugawara, T., Soga, R., and Yamase, I., J. Phys. Soc. Japan 19, 780 (1964).
31. Sugawara, T., and Yamase, I., J. Phys. Soc. Japan 18, 1101 (1963).

32. Thoburn, W. C. Magnetic properties of Gd-La and Gd-Y alloys. Unpublished Ph.D. thesis. Ames, Iowa, Library, Iowa State University of Science and Technology. 1956.
33. van Vleck, J. H. The theory of electric and magnetic susceptibilities. 1st ed. London, Oxford University Press. 1932.
34. Weiss, P., J. Phys. 6, 667 (1907).
35. Zener, C., and Heikes, R. R., Revs. Mod. Phys. 25, 191 (1953).

VII. ACKNOWLEDGEMENTS

The author wishes to thank Dr. D. K. Finnemore for suggesting this problem and for guidance and encouragement through all aspects of the work.

In addition, he would like to express appreciation to Dr. T. F. Stromberg and Mr. H. H. Sample for many helpful suggestions. Thanks are also due to Dr. F. H. Spedding and Mssrs. B. J. Beaudry and P. E. Palmer for preparing the samples.